ADDIS ABABA UNIVERSITY
SCHOOL OF GRADUATE STUDIES
SCHOOL OF EARTH SCIENCE

DEFORMATION, METAMORPHIM AND TECTONICS OF THE PRECAMBRIAN ROCKS OF ATSBI AREA, TIGRAY, N. ETHIOPIA

BY
TAMRAT MEKURIA

A thesis submitted to School of Graduate Studies of Addis Ababa University, in partial fulfillment of the requirements for the degree of Master of Earth Science (Structural Geology)

Jun 2014

ADDIS ABABA UNIVERSITY
SCHOOL OF GRADUATE STUDIES
SCHOOL OF EARTH SCIENCE

DEFORMATION, METAMORPHIM AND TECTONICS OF THE PRECAMBRIAN ROCKS OF ATSBI AREA, TIGRAY, N. ETHIOPIA

BY
TAMRAT MEKURIA

ADVISOR: MULUGETA ALENE (PhD)

A thesis submitted to School of Graduate Studies of Addis Ababa University, in partial fulfillment of the requirements for the degree of Master of Earth Sciences (Structural Geology)

Jun 2014

ADDIS ABABA UNIVERSITY
SCHOOL OF GRADUATE STUDIES
SCHOOL OF EARTH SCIENCE

DEFORMATION, METAMORPHIM AND TECTONICS OF THE PRECAMBRIAN ROCKS OF ATSBI AREA, TIGRAY, N. ETHIOPIA

BY
TAMRAT MEKURIA

APPROVED BY EXAMINING BOARD	**SIGNATURE**
Department Chairman and Graduate committee	
Dr. Seifu Kebede	________________
Advisor	
Dr. Mulugeta Alene	________________
Examiners	
Dr. Tesfaye Kidane	________________
Dr. Bekele Abebe	________________

Jun 2014

ACKNOWLEDGMENT

I would like to deeply thank Addis Ababa University, school of Earth Science for funding this project, providing thin section and microscope lab. I am very grateful of Dr Mulugeta Alene, my Advisor, who gave me valuable advice, constructive comment, suggestion, and for his continuous guidance with good sense of responsibility and personality and also for his valuable technical discussion and encouragement I have had without any reservations.

I run out of words to express my deepest thank to Ato Abebe Bedassa for all support I had from him. He is the one who help me for funding budget for the geochemistry analyzed in Ethiopian geological survey central laboratory.

My sincere gratitude goes to the thin section expert Ato Woldesilassie and Ato Wondowessen who helped me in thin section preparation. The contribution of my colleagues from other department in Arc GIS and other software is highly acknowledged.

My greatest appreciation also goes to my dear parents, colleagues and friends for their reading, technical editing, valuable comments and support.

Last but not least, thanks are also extended to the community of Atsbi town for their unforgettable support and helped me during field work to carry out the field mapping go smoothly.

TABLE OF CONTENT

LIST OF FIGURE

LIST OF TABLE

LIST OF APPENDIX

ABSTRACT

The Tsaliet Group of Atsbi area is covered by widely distributed basement rocks of both metavolcanic and metavolcaniclastics rocks and Phanerozoic sandstone. The study area is represented by extensively exposed metavolcaniclastic rocks consisting of metabreccia, tuffaceous layers and slate units and metavolcanic rocks consisting of metabasaltic andesite and meta-andesitic units. These low grade rocks show N-S regional trend and they are presumably correlate with similar Neoproterozoic rocks of Arabian Nubian Shield.

The Atsbi area is one of the area where tectonic structures are recorded by the Tsaliet Group that related to the collision history of ANS. Poly phase deformations in rocks of the study area are marked by the existence of different types of structural element such as regional pervasive foliation, superimposed folds, various lineation and brittle structure such as joints. Two phases of ductile deformation (D1 and D2) and one phase of brittle deformation (D3) are recognized. D1 deformation phase is related to N-S compression that resulted in a pervasive foliation, sub vertical to vertical folds and lineation whereas D2 deformation produced open, upright and harmonic low plunging folds and lineation. The brittle structures such as joints that crosscut the regional foliation represent the younger (D3) deformation phases of the area.

Field and petrographic observations show that the metavolcanic rocks are locally affected by propylitic alteration and sericitization. The metavolcanic rocks locally experienced pervasive silicification, sericitization, chloritization and epidotization. The critical minerals such as tremolite/actinolite, epidote, chlorite, sericite, muscovite, calcite demonstrate lower green schist facies of metamorphism of the study area.

The geochemical result from the metavolcanic rocks of Atsbi area show a small range of composition indicating that they may have originated from a single, chemically uniform parent melt. The metavolcanic rocks are principally identified as low-silica andesite and only a few samples fall in the basaltic andesite field. The mafic/intermediate rocks also show predominantly calc-alkaline affinity and The Zr-Nb-Y diagram shows that all the metavolcanic rocks lie within plume tholeiites volcanic arc basalt field.

CHAPTER ONE

1. INTRODUCTION

1.1 Background Information

The Late Proterozoic rocks of NE Africa (Saudi Arabia, eastern Egypt, eastern Sudan) record a succession of mild collisions resulting from the successive accretion of island arcs (Shackleton, 1986). McWilliams (1981) argued that Gondwanaland was assembled during the Neoproterozoic from two fragments - East and West Gondwanaland along the Pan-African Mozambique Belt of East Africa. This suggestion is supported by the lithologic associations characteristic of the Mozambique Belt and its extension to the north, the Arabian-Nubian Shield (ANS).

The basement in northeast Africa and Arabia is referred to as Arabian Nubian Shield predominantly juvenile continental crust formed by differentiation of mantle melts largely without reworking of preexisting continental crust (Stern, 1994). The ANS represents the northern part of EAO which formed by collision between East and West Gondwana at the end of a Wilson cycle. Geochemical and isotopic signatures indicate that these rocks are dominantly mantle-derived juvenile crust (Stern, 1994, 2002). The shield is dominated by supracrustal metavolcanics including volcaniclastics and immature sediments mostly metamorphosed in the green schist facies, variously deformed and intruded by granites, gabbros, and dikes. It extends from Jordan and Israel in the north, through to Ethiopia and Sudan in the south (Berhe, 1990; Kroner et al., 1991; Stern, 1994; Teklay et al., 1998, 2001). In Ethiopia, the ANS merges with the Mozambique Belt which is the southern half of the EAO and which accommodated the most intense collision between East and West Gondwana fragments (e.g. Stern, 1994).

The Northern metamorphic terrain of Ethiopia (Figure 1.1) is represented by a series of thick, inhomogeneous volcano-sedimentary assemblages, which belong to the Arabian Nubian Shield (ANS) sector of the East Pan-African orogen (Tadesse et al., 1999; Asrat et al., 2001).

The stratigraphy of the Late Neoproterozoic low-grade metasediments of Tambien Group and metavolcanics of Tsaliet Group of north Ethiopia was described by (Beyth, 1971, 1972; Garland, 1980; Kazmin, 1973). As it is summarized by Tadesse (1997), the previous authors describe the Precambrian geology of northern Ethiopia belongs to two major stratigraphic groups: the Tsaliet Group and the Tambien Group with minor but locally important and younger stratigraphic formation; namely the Didikama formation, the Shiraro formation and Matheows formation in younging stratigraphic sequence.

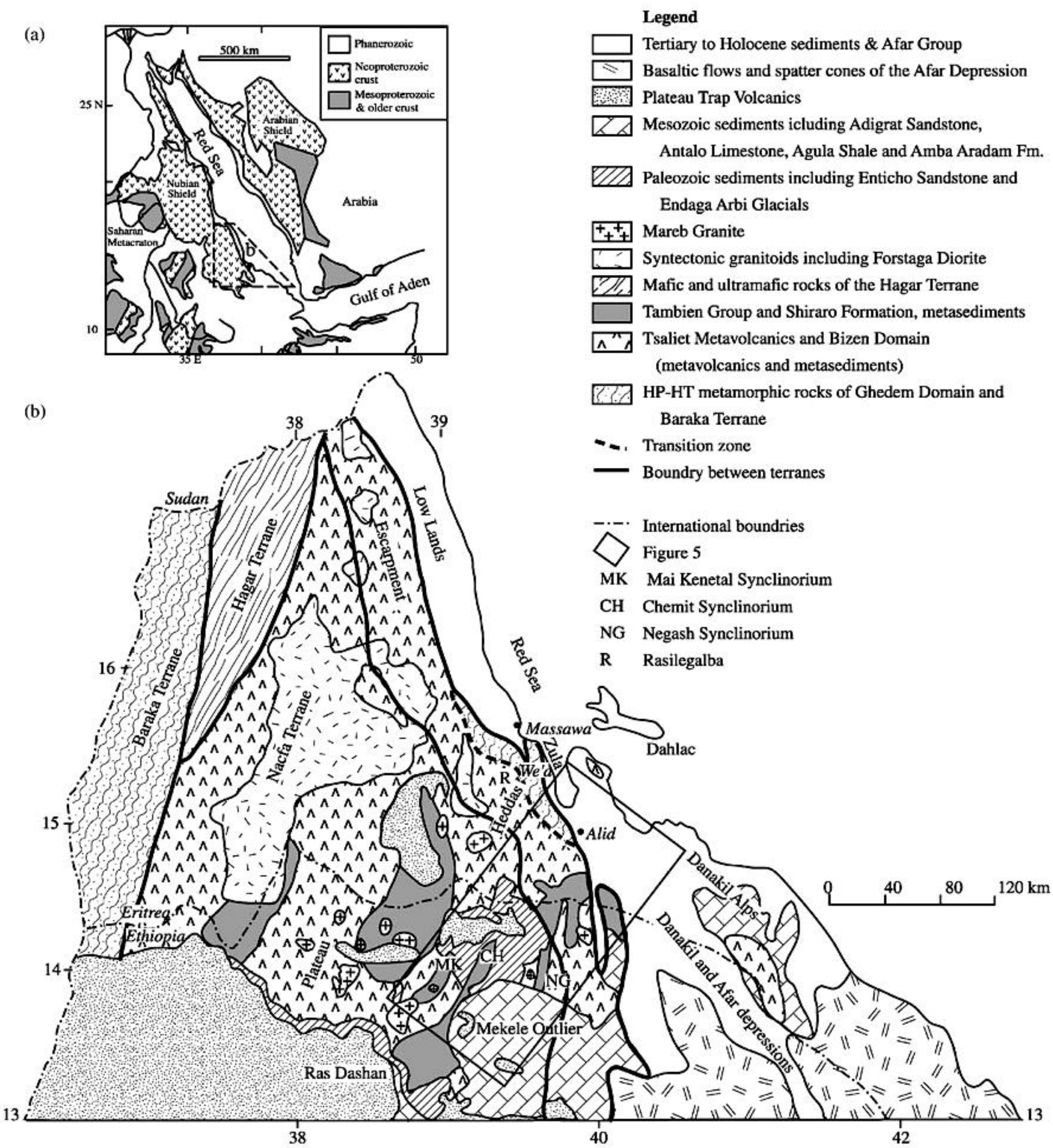

Figure 1.1 Location map and generalized geological map of northern Ethiopia and Eritrea (After Beyth et al., 2003).

The Tambien Group are predominately a metasediments distributed in the Mai kenetal, Tsedia, Chehmit, Negash, Halagubi synclinoria, Shiraro area and Escarpment East of Edaga Hamus (Beyth, 1972 and Sifeta el al., 2005). The Tsaliet metavolcanics composed of Green schist which were originally volcanic rocks, quartz schist originally rhyolitic volcanics and rocks cut by dolerite to quartz diorite intrusions and later by quartz porphry. The Tsaliet Group are unconformably overlain by the metasediments of Tambien Group but the lower boundary is not exposed (Beyth, 1972). The Atsbi horst is one of the area where the Tsaliet Group is exposed. Regionally the Tsaliet metavolcanic unit is the least studied as compared to the Tambien Group which get many attention by many researcher. The data presented in this research will help further to understand the least studied Tsaliet Group.

1.2 Location and Accessibility of Study Area

Tigray is the northern province of Ethiopia and one of the historical regions of the country where ancient cities, religious place and monument like Axum are found. Atsbi is situated in Tigray region on the northern part of the Ethiopia just to the west of the Ethiopian - Afar Rift Valley at the central east of Wikro map sheet (1339 B1). The study area cover 42 Km^2 and is located around 67 km from Mekele town, capital of the Tigray National state. It is bounded by UTM coordinates of 579000 E to 573000 E and 1530000 N to 1537000 N (Figure 1.2).

The study area can be reached using daily flight from Addis Ababa up to Mekele town then can be used by four wheel drive vehicle from Mekele to Atsbi or by using the main highway Addis Ababa – Mekele – Adigrat, through towns such as, Debrebirhan, Desse, Woldiya and Alamata in the northeast direction. From Addis Ababa to Wikro it can be accessed through Asphalt road whereas from Wikro to Atsbi, it is all weather gravel road. Footpaths connecting villages are common in the mapping area, which are very important in facilitating to get back to town from field travel.

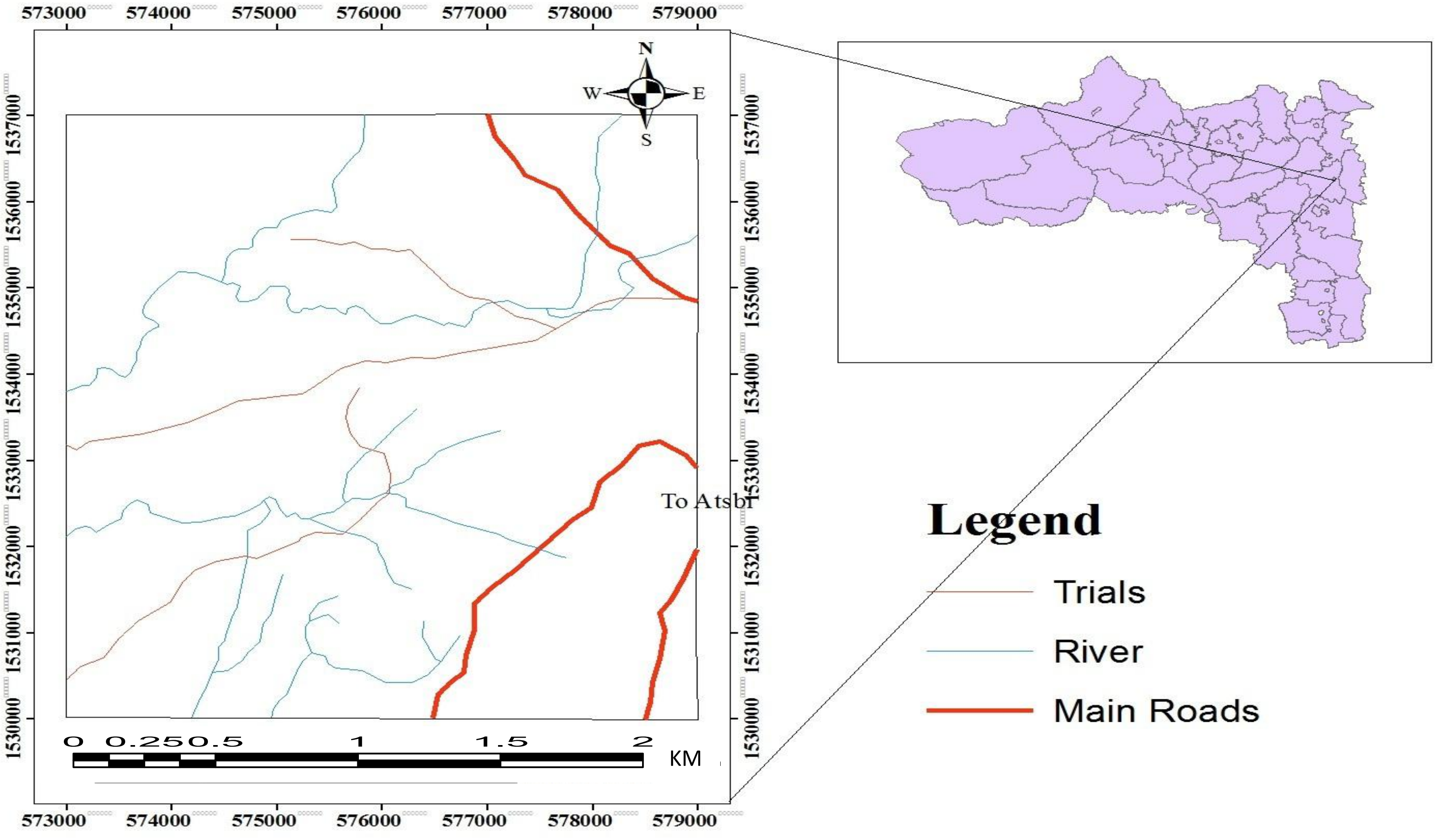

Figure 1.2 Location map of the study area

1.3 Physiography and climate

The map area have topographic expression of elongated ridges trending north east to north west direction on its most central part the study area with sporadic small ridges, prominent hills and deeply incised valleys in the western and eastern parts. There is no remarkable elevation difference, the maximum altitude recorded at the study area being 2,759m and the lowest is less than 2,612m above mean sea level. Some small creeks and valleys (most of them dry) are observed in the area but in the western side there is a big river called Hidar river that flows to the south west.

The region is known to have arid to semi arid climatic condition with the average rainfall of 600 mm to 800mm and average annual average temperature of 25^0c (Garland, 1980). The region received high rainfall from mid June to mid September within a year. The area is solely populated by Tigrigna speaking, Tigre people. Amharic is second language spoken. In the study area it can be said that the area is scarcely populated even if the population density varies from place to place. This population distribution and density is controlled by availability of water, farming land and accessibility to the nearby town.

1.4 Objective of the Study

1.4.1 General objective

The general objective of this study is designed to explain different geological structure and their deformation phases, various lithologic unit of the area with their related metamorphic evolution and to understand the regional tectonic domain of the region.

1.4.2 Specific objectives

- Production of a geologic map of the study area at scale of 1:25,000
- To recognize the sequential development of structures (phases of deformation) and establish the relationships between lithology and metamorphism by analyzing metamorphic microstructure using thin section.
- Description and analysis of macro and micro scale geologic structure of the area like folds, foliations and joints

- Petrographic analysis of representative sample from each units of the Atsbi area, to determine the mineralogical composition.
- To attempt to relate the geology of the study area with respect to local and regionally known tectonic domains using geochemical analysis (major, minor and trace elements) by XRF method

1.5 Significance of the Study

Neoproterozoic sequence is one of the least studied in Africa, yet lies at a critical geotectonic boundary between the Arabian–Nubian Shield (mostly juvenile crust) to the north and Mozambique belt (mostly reworked older crust) to the south (Alene et al., 2006). The metamorphic terrane of northern Ethiopia is also one of the least studied areas in eastern and northeastern Africa. Regional mapping of parts of the geology of northern Ethiopia by Levitte (1970), Beyth (1971, 1972) and Garland (1980) and compilation work of the geology of Ethiopia by Kazmin (1973) remain as standard references to the geology of the region. Therefore, it is believed that this study basically helps to improve the existing knowledge on the Tsaliet Group by providing local lithologic data, structural data and to some extent geochemical data to support the regionally identified tectonic domain of the Tsaliet Group.

1.6 Methodology

Before deployed to the field office preparation has been undertaken. This include review of previous work and available maps in order to have an overview about the geology of the area and surrounding region, aerial photos are examined and interpreted using table stereoscope, requesting field material and equipment from Addis Ababa university store and other preparatory works has been accomplished.

1.6.1 Field work

During the course of mapping, lithologic, structural mapping and sampling has been undertaken. The traverses were designed across the structure or regional foliation and denser traverse lines and observation points were taken where the exposure of the rock are clear and abundant. Accordingly nine traverse line were selected that potentially targeting to cross the regional structure or foliation. Observation point were made depending on the change on the lithology or structural complexity.

In the field different rock formations and their relationship to the other formations were observed. Description of lithostratigraphy in relation to measurement, observation and recording of all structural data have been undertaken. Description of all the lithological variation in color, texture, mineral composition, kind and degree of weathering, color of fresh surface, fabric and etc have been done. Quartz veins that possibly occur in a sequence of metamorphic rocks in the study area with their aerial extent, attitude and contact relationship were also examined and noted in the field for further analysis. Interpretation of rocks was mainly done on site by visual observation using hand lenses.

About 25 representative rock samples were systematically collected for petrographic and geochemical studies from some appropriate locations. Finally, fair copy of tentative geological map was produced in the field. Throughout all traverses photos are taken for all lithologic and structural elements by digital camera that facilitates the whole thesis work after being returned from the field.

1.6.2 Post field work

The field data (structural, lithologic and mineralization) after being compiled were analyzed after returning from the field.

1.6.2.1 Petrographic Analysis

Petrographic study including mineral identification and fabric/microstructural analysis was carried on thin sections laboratory at school of Earth science in Addis Ababa university. The results of petrographic studies of the thin section were used to clear the doubts of field naming of the rocks, identify metamorphic mineral assemblage and the grades of metamorphism of the area. Furthermore, it is used to explain the relationship between deformation and metamorphism and study microstructure in order to support idea that the study area have been experienced polyphase deformation based on the field record and mapping.

1.6.2.2 Structural data analysis

Field mapping and data collection of each structural elements such as folds, foliation, lineation and joints were conducted from each units without data selection and those data are analyzed by using different methods. Field information was compiled using Arc GIS software to generate detail geological map at scale of 1:25,000, which shows lithological units and orientations of major geological structures. Stereonet (version 9.0.2) is used to analyze each structural elements associated with each phase of deformation individually and also used to illustrate structural and geometric relationships. To get an overall orientation of the foliations, folding and fractures, the poles of these planes have been plotted and contoured on the Stereonet.

1.6.2.3 Geochemical analysis

Chemical analysis of rock samples that showed the least signs of weathering and deformation, from visual as well as from thin section observations, was carried out at the geochemical laboratory of the Geological Survey of Ethiopia central laboratory. The samples are analyzed for major, minor and trace element geochemical analysis using Philips X-ray fluorescence spectroscopy model PW 2400 in Addis Ababa. During sample collection particular care has been taken to ensure that the sample is fresh. The data's are then plotted and analyzed by using different diagrams using Petrograph 2beta software.

1.7 Review of Previous Work

The Precambrian contains a wide variety of sedimentary, volcanic and intrusive rocks which have been metamorphosed to varying degrees (Mengesha et al., 1996). These rocks were given formal stratigraphic names and were correlated with low grade rocks of western and southern Ethiopia and were recognized to the upper complex division of three fold classification of the Ethiopian basement rocks by Kazmin (1973). Many geological work in the basement of northern Ethiopia have been done for the last decades that identified and mapped extensive low grade Precambrian basement rocks comprising metavolcanic, metasediments and intrusive of varied composition (Levitte, 1970; Beyth, 1972; Garland, 1980).

The Neoproterozoic basement of central Tigrai, northern Ethiopia is composed of low-grade metavolcanics, slate, carbonates and plutonics (Arkin et al., 1971; Beyth, 1971; Garland, 1980; Alene, 1998). Others authors try to describe the northeast Ethiopian plateau as a low-grade metamorphic complex which includes the Tsaliet Metavolcanics overlain by the NE-trending upright folded metasediments of the Tambien Group (Beyth e al., 2003). The basement is overlain by flat-lying Phanerozoic sediments and volcanics. The metamorphic grade of the Tsaliet Metavolcanics and the Tambien Group is low and, except around intrusions, never rises above greenschist facies (Alene, 1998; Alene and Sacchi, 2000; Beyth e al., 2003).

The northern basement of Ethiopia is in the south (Nafka terrane) of the Arabian–Nubian Shield (ANS) that developed during the Neoproterozoic by rifting, arc accretion and terrane amalgamation processes in the East African Orogen (Stern, 1994; Johnson and Woldehaimanot, 2003). The ANS (Figure 2.4) is one of two major terranes in north and east Africa that developed during the Neoproterozoic (Kroner, 1980; Stern, 1994). Many authors consider the ANS to be juvenile arc crust formed during the closure of the Mozambique Ocean during assembly of east and west Gondwanaland in Neoproterozoic time, forming the East African Orogen (Berhe, 1990; Abdelsalam and Stern, 1996; Stern, 1994, 2002; Kroner and Stern, 2005).

Geochemical and Nd, Sr, and Pb isotope characteristics of the rocks of this terrane indicate that they resulted from accretion of intra-oceanic island arcs composed of juvenile Neoproterozoic crust, which is mainly derived from a depleted mantle source (e.g. Kröner et al., 1991; Stern, 1994; Stern, 2002; Tadesse et al. 1999, 2000; Teklay et al., 2002; Gebresilassie, 2009). The chemistry of the volcanic rocks in some northern Ethiopian district is characteristically calcalkaline, and most yield arc-related geochemical signatures. Such calcalkaline volcanic activity, post-orogenic granitoids and deposition of clastic rocks are common in the juvenile crust of the ANS (Sifeta et al., 2005)

The basement rocks of Ethiopia have long been considered to be part of the Arabian–Nubian Shield (Kazmin et al.,1978; Tadesse et al., 1999; Asrat et al., 2001). The Tsaliet Metavolcanics of north Ethiopia (Figure 1.1) which covers the greater part of the basement of Tigrai is formed by a heterogeneous series of rocks with obvious volcanic association (Beyth, 1972; Garland, 1980). These group of rocks are equivalent to the metavolcanics of the Bizen Domain in east Eritrea and are mainly formed of intermediate to felsic and welded tuffs, well-bedded lapilli tuffs and agglomerates, and limestone in the section upper parts (Beyth, 1972).

The structure of the basement complex is defined by NE-trending folds with NW-dipping bedding and foliation on the plateau, and SE-dipping structure in the Ethiopian escarpment area (Beyth et al., 2003). The tectonic structures recorded by the Tsaliet and Tambien Group rocks are related to the collisional stress that resulted in the amalgamation of the ANS. Generally, two phases of deformation (D1 and D2) are recognized (Alene et al., 2006). Deformation D1 is caused by N-S compression and resulted in tight minor folds with a wavelength of several mm to dm, elongation lineation and pervasive regional foliation (Alene et al., 2006). D2 deformation resulted from E-W directed compression at the waning stage of the collision between East and West Gondwana and yielded long wave length (about 8 km), upright, open parallel folds without a significant cleavage, thrust, and strike slip faulting (Alene et al., 2006).

CHAPTER TWO

2. REGIONAL GEOLOGY

2.1 Regional Geologic setting

2.1.1 Pan African Orogeny

The term "Pan African" (loosely meaning " all Africa") was coined by Kennedy (1964) who recognized " an important and widespread tectonic and thermal event" which led to "structural differentiation of an original shied into croton and circum structural (orogenic) areas" about 500 Ma ago (Kroner, 1980). The Pan-African was also interpreted by other researchers as a tectono-thermal event, some 500 Ma ago, during which a number of mobile belts formed, surrounding older cratons. This thermal event was later recognized to constitute the final Part of an orogenic cycle, leading to orogenic belts which are currently interpreted to have resulted from the amalgamation of continental domains during the period 870 to 550 Ma. The term Pan-African is now used to describe tectonic, magmatic, and metamorphic activity of Neoproterozoic to earliest Palaeozoic age, especially for crust that was once part of Gondwana (Kroner and Stern, 2005).

Pan-African orogenic cycle is interesting in its own right. The nature of the episode supports arguments that modern plate tectonic systems had begun by about 1000 Ma (Stern, 1994). In contrast to crust produced between 1.0 and 1.8 Ga, Pan-African juvenile (i.e. mantle-derived) crust preserves most of the hallmarks of modern plate tectonic regimes, including abundant ophiolites, calc-alkaline batholiths and volcanic sequences, and immature elastic sediments. Horizontal tectonic displacements arc proved by ophiolitic nappes which traveled at least several tens and perhaps a few hundreds of kilometers (Stern, 1994).

Within the Pan-African domains, two broad types of orogenic or mobile belts can be distinguished. One type consists predominantly of Neoproterozoic supracrustal and magmatic assemblages, many of juvenile (mantle- derived) origin, with structural and metamorphic histories that are similar to those in Phanerozoic collision and accretion belts. Such belts include the Arabian-Nubian shield of Arabia and north-east Africa

(Figure 2.5), the Damara- Kaoko-Gariep Belt and Lufilian Arc of south-central and south-western Africa, the West Congo Belt of Angola and Congo Republic, the Trans-Sahara Belt of West Africa, and the Rokelide and Mauretanian belts along the western Part of the West African Craton. The other type of mobile belt generally contains poly deformed high-grade metamorphic assemblages, exposing middle to lower crustal levels, whose origin, environment of formation and structural evolution are more difficult to reconstruct. The protoliths of these assemblages consist predominantly of much older Mesoproterozoic to Archaean continental crust that was strongly reworked during the Neoproterozoic. Well studied examples are the Mozambique Belt of East Africa, including Madagascar (Figure 2.4) with extensions into western Antarctica, the Zambezi Belt of northern Zimbabwe and Zambia and, possibly, the little known migmatitic terranes of Chad, the Central African Republic, the Tibesti Massif in Libya and the western parts of Sudan and Egypt (Kroner and Stern, 2005).

Neoproterozoic closure of the Mozambique Ocean collapsed an accretionary collage of arc and micro-continental terranes and sutured East and West Gondwana along the length of the East African Orogen (Timothy et al., 2003). This suggestion is supported by the lithologic associations characteristic of the Mozambique Belt and its extension to the north, the Arabian-Nubian Shield (ANS). Following the arguments of Berhe (1990) suggesting ophiolite-decorated meridional sutures can be traced in East Africa, Stern (1994) accept these entities as along-strike correlatives, and refer to the larger structure as the East African Orogen (EAO; Figure 2.3).

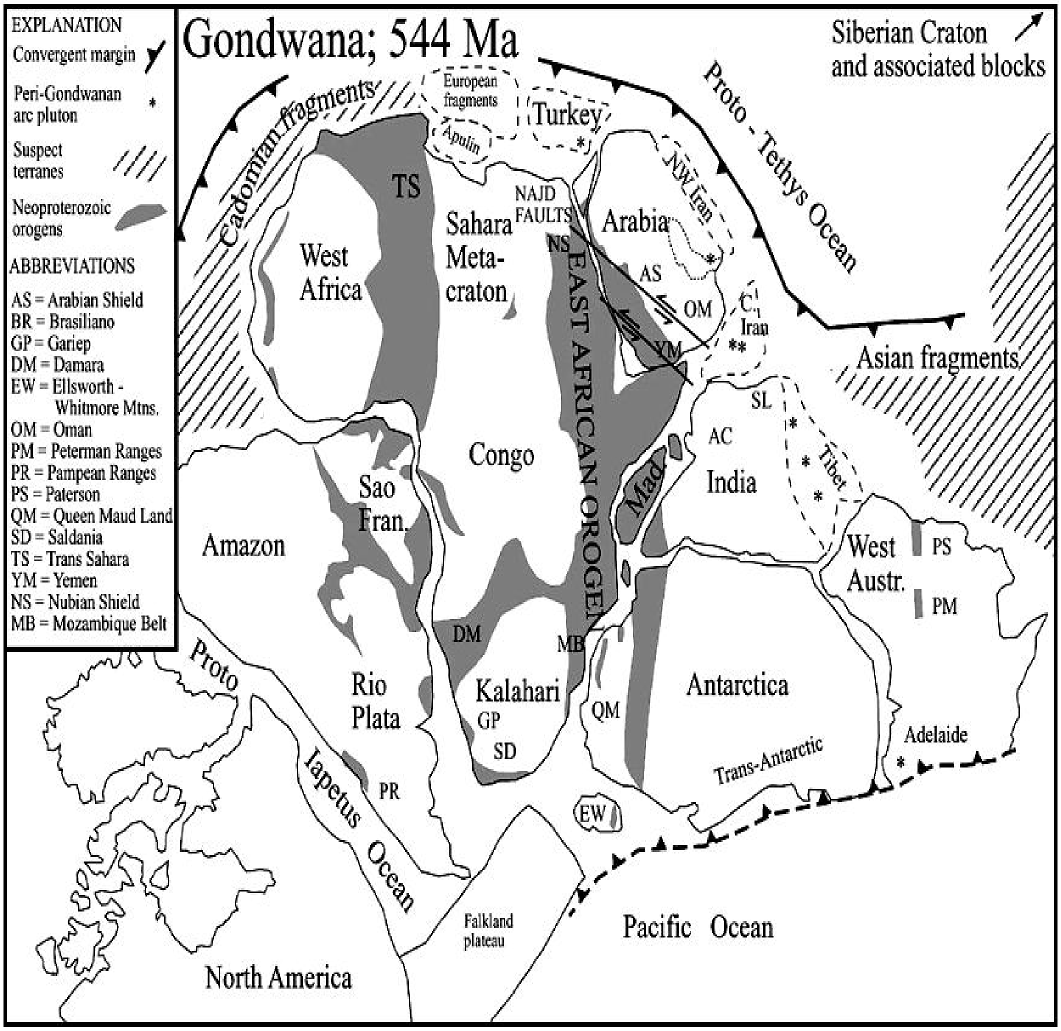

Figure 2.1 Map of Gondwana at the end of Neoproterozoic time showing the general arrangement of different tectonic elements (After; Timothy et al., 2003).

2.1.2 Geodynamic evolution of the East African Orogeny

The East African Orogen (EAO) is one of Earth's great collision zones, where East and West Gondwana collided to form the supercontinent 'Greater Gondwana' or 'Pannotia' (Figure 2.1) at the end of Neoproterozoic time (Stern, 2002). The ophiolites, granulites, and structures of the EAO are fossil fragments of a Neoproterozoic Wilson cycle, representing the opening and closing of an ocean basin that lay between the older crustal blocks of East and West Gondwanaland (Figure 2.2). Even if the understanding of the style and timing of collision between East and West Gondwanaland to form the East African Orogen is incomplete, the general outline of this important event in Earth history is slowly emerging (Stern, 1994).

According to Stern (1994) summarized in figure 2.2 the rifting as part of the breakup of Rodinia place in time about 850-900 Ma. In contrast, the sequence of events that begins with sea-floor spreading and formation of arcs and back-arc basins and continues with the accretion of these tectonic cells into juvenile crust is coming into sharper focus, at least for the Arabian-Nubian Shield. There is good evidence that these processes were underway as early as 870 Ma and continued until at least 690 Ma.

Accretion of numerous juvenile arcs and a few older continental fragments continued during this interval. Continental collision first led to crustal thickening and uplift, beginning perhaps as early as 750 Ma but certainly by 700 Ma, and continued with orogenic collapse and escape tectonics until the end of the Precambrian. At least as far as the EAO is concerned, this dates the consolidation of East and West Gondwanaland, although several oceanic basins of unknown dimensions persisted within West Gondwanaland.

Crustal thickening and uplift propagated with time eastward, now marked by zones of ~ 550 Ma granulites in southernmost India, Sri Lanka, and Madagascar. Tectonic escape led to the development of major rift basins in the northern EAO and environs which led directly to sea-floor spreading and formation of a passive margin on the remnants of Gondwanaland and the formation of an ocean basin to the north, at about 550 Ma ago.

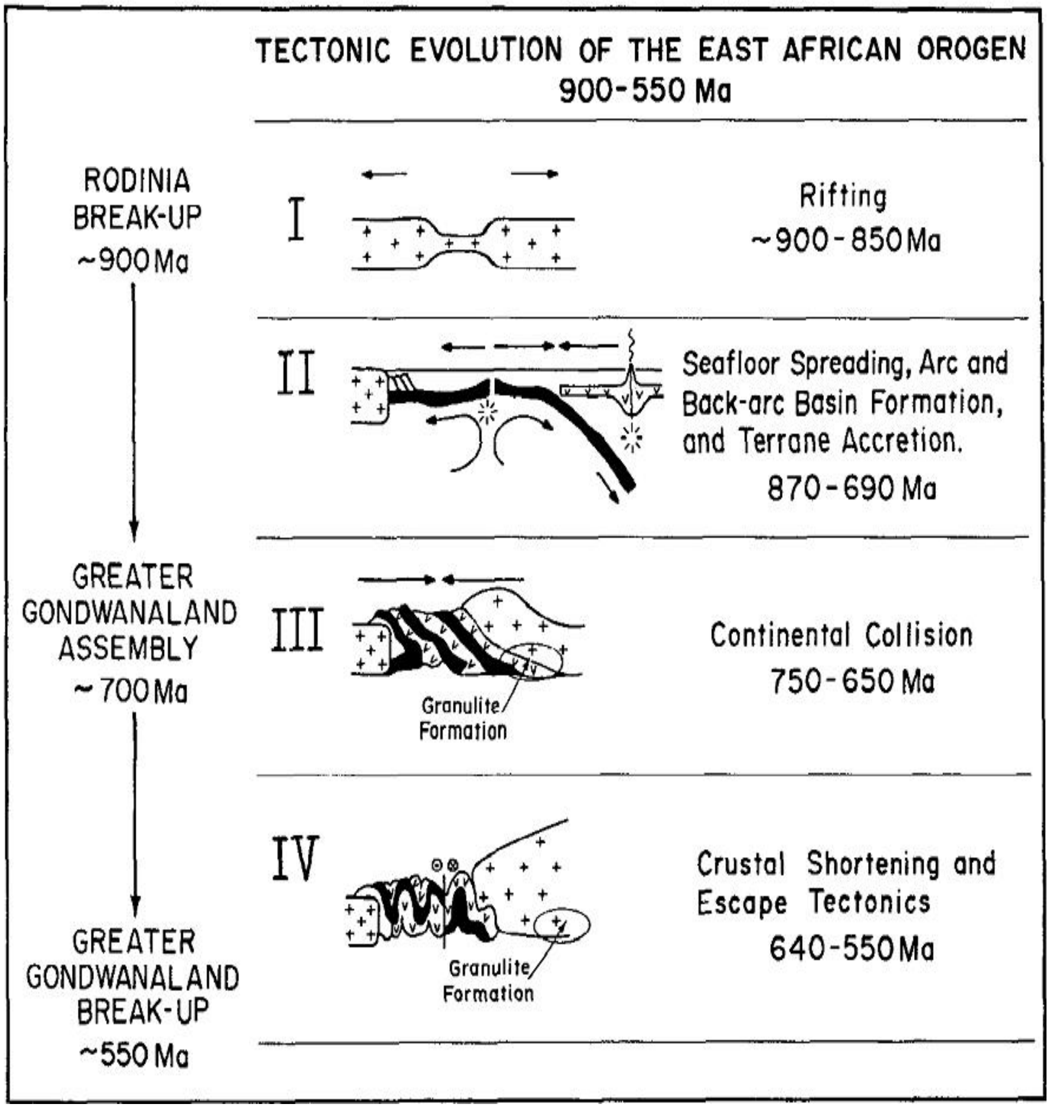

Figure 2.2 Two dimensional summery of the tectonic evolution of the East African Orogen (after; Stern, 1994).

Therefore the final collision between East and West Gondwana most likely followed the closure of the Mozambique Ocean, forming the East African Orogen (figure 2.3). The East African Orogen encompasses the Arabian–Nubian Shield in the north and the Mozambique Belt in the south (figure 2.3). These and several other orogenic belts are commonly referred to as Pan-African belts, recognizing that many distinct belts in Africa and other continents experienced deformation, metamorphism, and magmatic activity spanning the period of 800–450 Ma (Timothy et al., 2003).

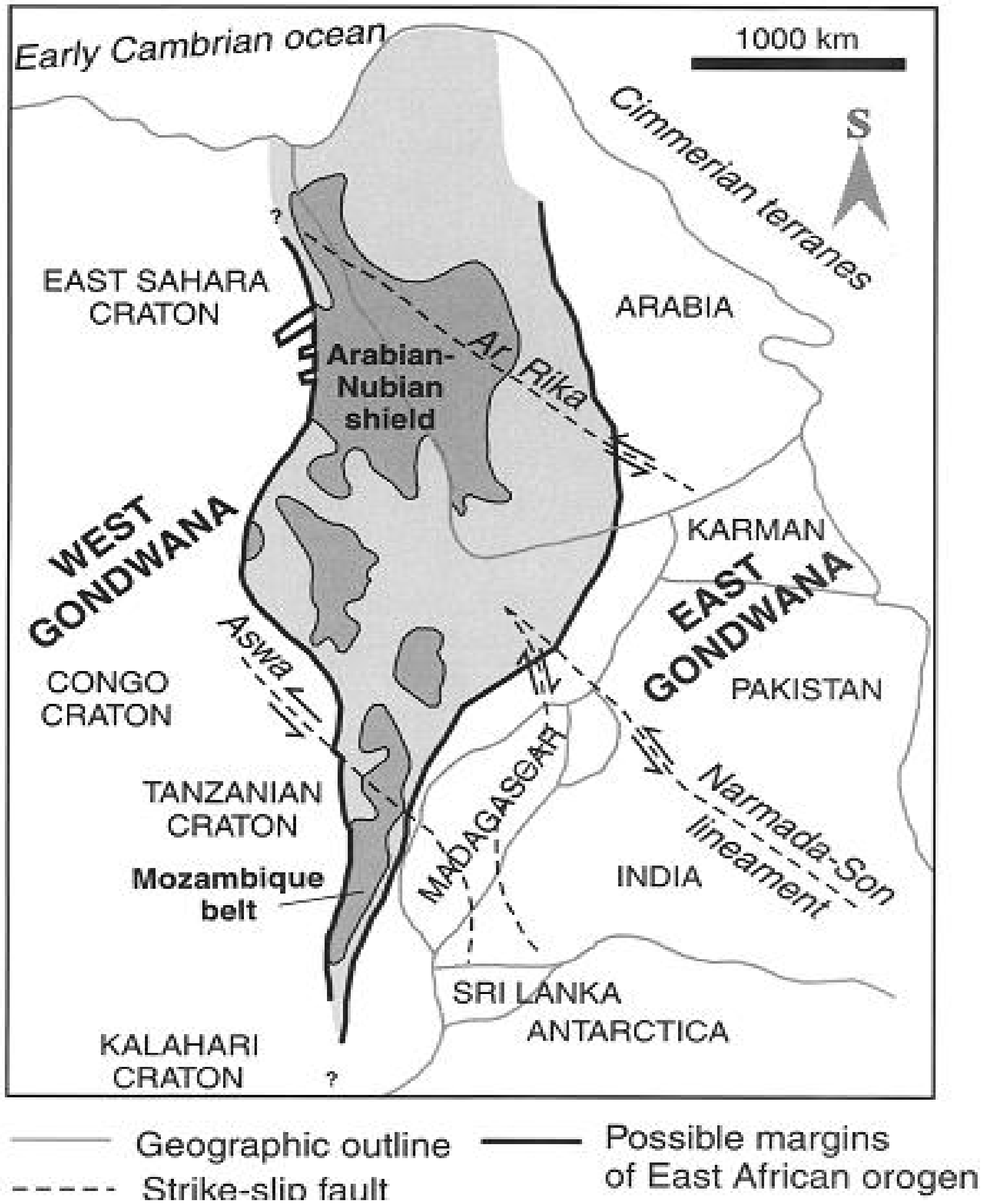

Figure 2.3 Sketch map of the East African Orogen showing the location of the Arabian-Nubian Shield relative to the mozambique Belt and adjacent cratonic margins (after Johnson et al., 2003)

2.1.3 Mozambique belt

Pan-African tectono-thermal activity in the Mozambique Belt was broadly contemporaneous with magmatism, metamorphism and deformation in the Arabian–Nubian Shield. The difference in lithology and metamorphic grade between the two belts has been attributed to the difference in the level of exposure, with the Mozambican rocks interpreted as lower crustal equivalents of the juvenile rocks in the Arabian–Nubian Shield (Timothy et al., 2003).

This broad belt defines the southern Part of the East African Orogen and essentially consists of medium- to high-grade gneisses and voluminous granitoids. It extends south from the Arabian-Nubian Shield into southern Ethiopia, Kenya and Somalia via Tanzania to Malawi and Mozambique and also includes Madagascar (see Figure 2.3) (Kroner and Stern, 2005).

2.1.4 Arabian Nubian Shield

A broad region was uplifted in association with Cenozoic rifting to form the Red Sea, exposing a large tract of mostly juvenile Neoproterozoic crust. These exposures comprise the Arabian-Nubian Shield (ANS). The Shield makes up the northern half of the East African orogen and stretches from southern Israel and Jordan south as far as Ethiopia and Yemen, where the ANS transitions into the Mozambique Belt (Figure 2.3). The ANS is distinguished from the Mozambique Belt by its dominantly juvenile nature, relatively low grade of metamorphism, and abundance of island-arc rocks and ophiolites (Kroner and Stern, 2005). The ANS, thus defined, extends about 3000 km north to south and >500 km on either side of the Red Sea (Figure 2.4).

Juvenile crust of the ANS was sandwiched between continental tracts of East and West Gondwana (Figure 2.3). The precise timing of the collision is still being resolved, but appears to have occurred after ~630Ma when high-magnesium andesite 'schistose dykes' were emplaced in southern Israel but before the ~610Ma post-tectonic 'Mereb' granites were emplaced in northern Ethiopia. By analogy with the continuing collision between India and Asia, the terminal collision between East and West Gondwana may have continued for a few tens of millions of years. Deformation in the ANS ended by the beginning of Cambrian time, although it has locally continued into Cambrian and Ordovician time farther south in Africa. The most intense collision (i.e. greatest shortening, highest relief, and greatest erosion) occurred south of the ANS, in the Mozambique belt. Compared to the strong deformation and metamorphism experienced during collision in the Mozambique belt, the ANS was considerably less affected by the collision (Kroner and Stern, 2005).

North-west trending left- lateral faults of the Najd fault System of Arabia and Egypt (Figures 2.3) formed as a result of escape tectonics associated with the collision and were active between about 630 and 560 Ma. Deformation associated with terminal collision is more intense in the southern ANS, with tight, upright folds, steep thrusts, and strike-slip shear zones controlling basement fabrics in Eritrea, Ethiopia, and southern Arabia. These north-south trending, collision-related structures obscure the earlier structures in the southern ANS that are related to arc accretion, and the intensity of this deformation has made it difficult to identify ophiolitic assemblages in southern Arabia, Ethiopia, and Eritrea. Thus, the transition between the ANS and the Mozambique Belt is marked by a change from less deformed and less metamorphosed, juvenile crust in the north to more deformed and more metamorphosed, remobilized older crust in the south, with the structural transition occurring farther north than the lithological transition (Kroner and Stern, 2005).

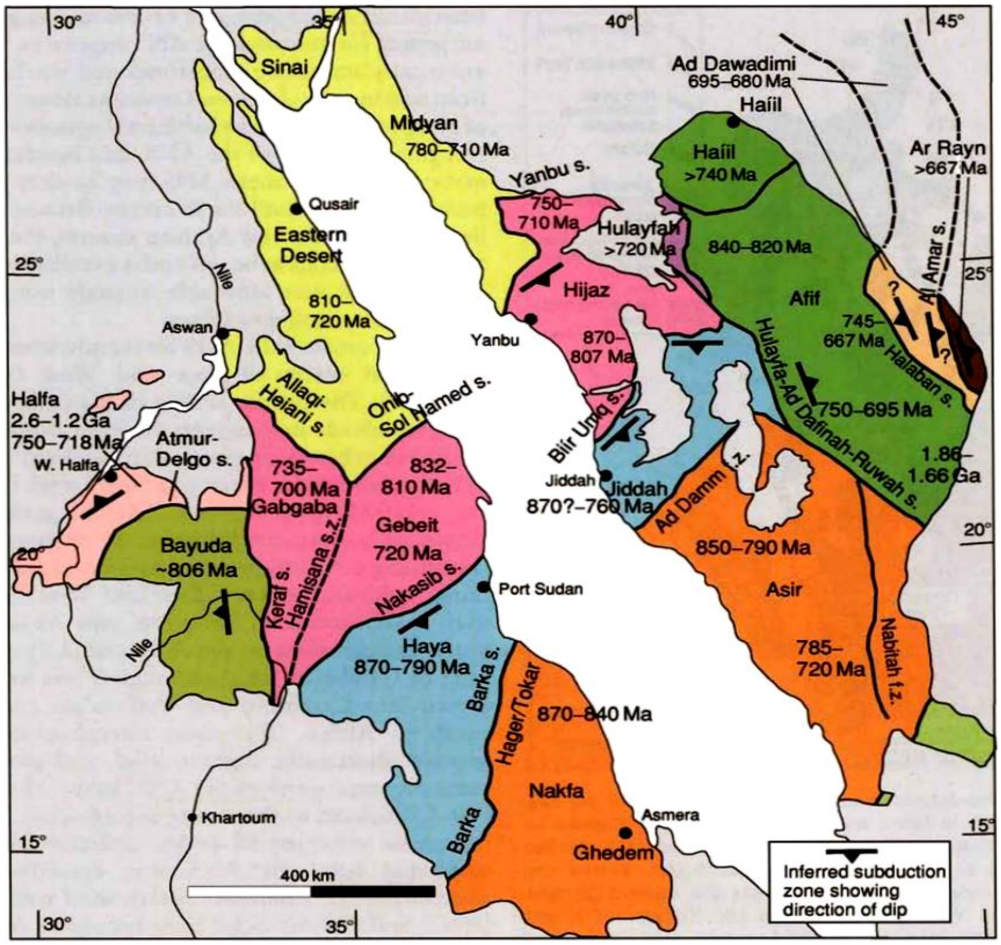

Figure 2.4 Terrain map of Arabian Nubian Shield. (After; Kroner and Stern 2005)

Abdelsalam and others describe the geology of this region, and relate it to events in the East African Orogen. They recognize three Neoproterozoic deformation events including early (700–650 Ma) emplacement of S- to SE-verging nappes consisting of ophiolites and passive margin sediments. E–W shortening produced by collision of the Saharan metacraton with the Arabian–Nubian Shield at 650–590 Ma formed N- to NE-trending folds in the eastern part of the craton. North to NNW-trending sinistral strike-slip shear zones developed at 590–550 Ma, and are kinematically linked to N-striking fold belts. North striking extensional shear zones may be related to late (post-550 Ma) extensional collapse of the orogen (Timothy et al., 2003). The final Stages in the evolution of the ANS witnessed the emplacement of post-tectonic 'A-type' granites, bimodal volcanics, and molassic sediments. These testify to strong extension caused by orogenic collapse at the end of the Neoproterozoic (Kroner and Stern, 2005).

2.2 Precambrian Geology of Ethiopia

The Precambrian shield in Ethiopia occupies a unique position in the African continent situated between the predominantly gneissic rocks of the Mozambique Belt, to the south in eastern and southern Africa, and the volcano-sedimentary- plutonic complexes along a strike to the north bordering, the Red Sea. The Orogenic belts of the Arabian Nubian Shield (ANS) and the Mozambique Belt (MB) are believed to be more prominent outcrop in Ethiopia than in any other country of the Horn of Africa. Studies of the basement reveal important features in the development of both belts (Kazmin, 1972; Berhe, 1990; Kazmin et al., 1978).

Precambrian rocks exposures are found in areas not intensively affected by Cenozoic volcanism and rifting and where the Phanerozoic cover rocks have been eroded away. These rocks outcrop in four major regions around the plateau margins: Tigray - Northern Ethiopia, Gojjam, Wollega, Illubabor and Kefa - West and Southwest, Sidamo & Bale - South, Hararghe- East (Mengesha et al., 1996). The basement comprise high-grade ortho- and paragneisses and migmatites, low-grade volcano-sedimentary, ultramafic assemblages and granitoids of variable composition (Yibas et al., 2002). Kazmin(1971, 1973 and 1978) tried to classify the Precambrian rocks in his three fold classification as the Lower, the Middle and the Upper Complexes based on mainly on metamorphic grade and deformational differences. The lower complex comprises various high grade gneisses and migmatites. Biotite and amphibole gneisses predominate, with subordinate quartzo- feldspathic gneisses, calc-silicates and amphibolites. The middle complex represented by psammitic and pelitic metasediments (biotite and quartz muscovite schists, meta-arkoses, quartzites) with subordinate marbles, calc-silicates and amphibole schists. The Upper Complex consists of low-grade rocks in following succession: ophiolitic rocks, andesitic metavolcanics and associated metasediments, clastic and to less extent carbonate sediments (Kazmin 1971, 1973; Garland,1980). Although, this threefold classification by Kazmin was used as base map for other recent researcher, the validity of the classification has been challenged recently following U–Pb zircon dating of various gneisses (Ayalew et al., 1990; Teklay et al., 1998; Yibas et al., 2002; Asrat et al., 2001).

Generally, the Ethiopian basement have been studied by several researchers. Starting from the first systematic mapping done in the northern part of the country by Dainelli & C. Marinelli (19120); G. Marle & E. Minucei (1938); Dainelli (1943) as sited by Beyth (1971). For the past decades some researchers provided good researches that help to understand the Ethiopian basement. Some of them from the past to the recent are: Levitte (1970), Kazmin (1971, 1973), Kazmin et al. (1978), Beyth (1971, 1972), Garland (1980), de Wit and Chewaka (1981), Ayalew et al. (1990), Mengesha et al., (1996), Tarekegn (1997), Tadesse et al. (1997, 1999, 2000), Alene (1998), Alene et al.(2000, 2006), Asrat et al. (2001, 2004), Yibas et al.(2002), Miller et al.(2003,2009, 2011) and Avigad et al.(2007).

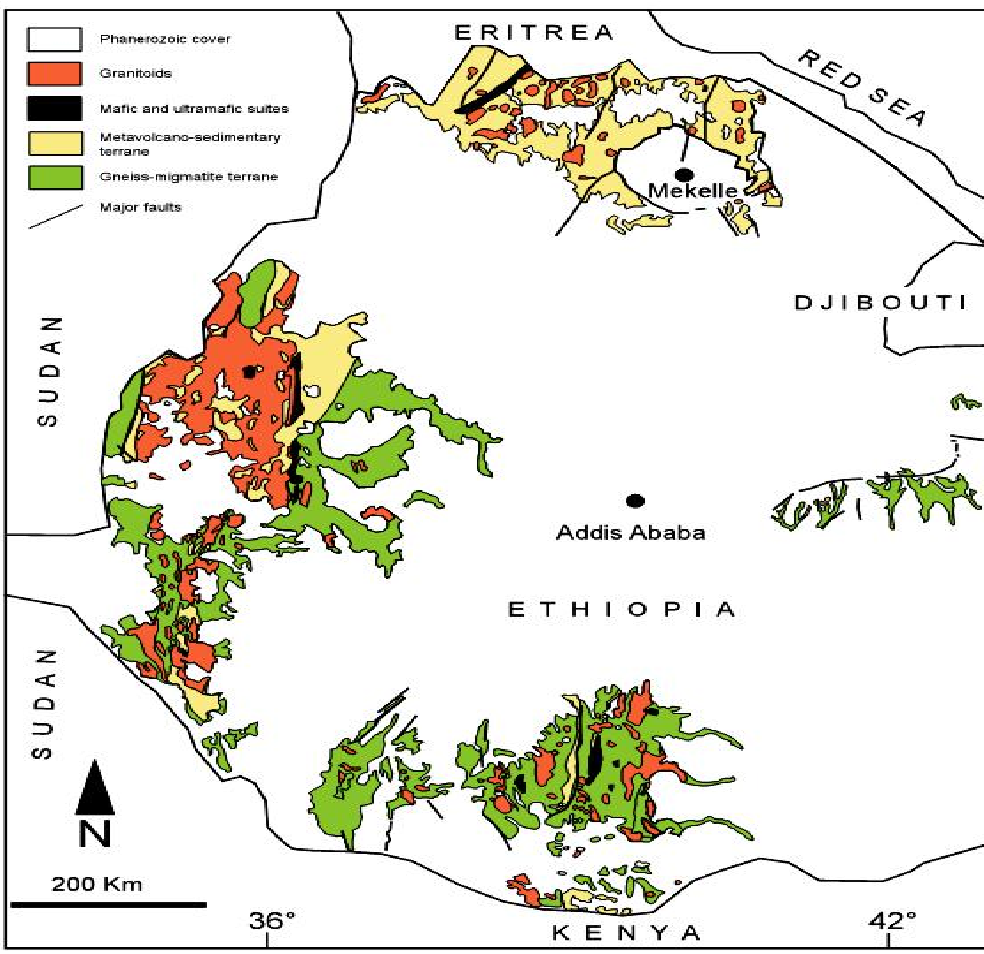

Figure 2.5 Distribution of the low grade volcano-sedimentary sequences of the ANS and high grade gneisses and migmatites of the Mozambique belt in Ethiopia (modified from Asrat et al., 2001 sited by Gebresilassie, 2009)

2.2.1 Precambrian rocks of Northern Ethiopia

The Neoproterozoic basement of Ethiopia lies at the transition between the northern and southern sectors of the East African Orogen. It is compositionally similar to juvenile ANS crust but its structure is dominated by N–S trending “shortening zones” more common to the south (Abdelsalam and Stern, 1996). The Northern metamorphic terrain of Ethiopia (Figure 1.1) is represented by a series of thick, inhomogeneous volcano-sedimentary assemblages, which belong to the Arabian –Nubian Shield (ANS) sector of the East Pan-African orogen (Tadesse et al., 1999; Asrat et al., 2001).

The first recorded geological work in the northern province of Ethiopia was done by Blanford (1870) as sited by Beyth (1971). After this time different geological mapping were carried out by different researchers and identified and mapped extensive low grade Precambrian rocks composed of metavolcanic, metavolcaniclastics and metasediments including intrusive rocks of varied composition (Beyth, 1972; Kazmin, 1972; Garland, 1980). Tarekegn (1997), try to summarize the basement rocks using previous works and Kazmin (1972), indicating most parts of Precambrian geology of northern Ethiopia belongs to two major stratigraphic groups: the Tsaliet Group and the Tambien Group with minor but locally important and younger stratigraphic formation; namely the Didikama formation, the Shiraro formation and Matheows formation in younging stratigraphic sequence.

The Tambien Group is exposed throughout portions of northern Ethiopia (Tigre Province) and Eritrea (NNE extensions from; Bizen domain and Adobha Abi terrane of Beyth et al. (2003), in green schist-grade terranes comprising the southern portion of the Arabian –Nubian Shield (Miller, 2011). The Tambien Group are predominately a metasediments distributed in the Mai kenetal, Tsedia, Chehmit, Negash, Halagubi synclinoria, Shiraro area and Escarpment East of Edaga Hamus. This unit unconformably overlain by Enticho sandstone and Edaga Arbi glacial but the contact relationships between these two Groups is still undifferentiated, however it will ranging from probably unconformable to gradational and fault bounded (Beyth, 1972 and Sifeta el al, 2005).

The Tsaliet metavolcanics are building the Tsaee anticlinorium and the area west of mai kenetal synclinorium, the Bereh anticlinorium and another overturned anticline west of Negash synclinorium. The Atsbi horst and most of the Escarpment area around Berahle are included. This group composed of Green schist which were originally volcanic rocks, quartz schist originally rhyolitic volcanics and rocks cut by dolerite to quartz diorite intrusions and later by quartz porphry. The Tsaliet Group are unconformably overlain by the metasediments of Tambien Group but the lower boundary is not exposed (Beyth, 1972). The Tsaliet metavolcanic may be correlated with the Adola series of southern Ethiopia and the Halaban formation of Saudi Arabia although the metamorphic grade is lower than in the Adola series and the intrusion are not ultrabasic but, mainly dioritic and granodioritic as in Halaban formation. The Tambien is correlative with the Murdama formation of Arabia and the Uda-Ad of Somali land which are overlain by the unmetamorphosed conglomeratic volcanic complex of Fatima formation which is Eocambrian in age (Beyth, 1972).

The metamorphic sequence in the Mekele – Adigrat area is composed dominantly of heterogeneous metavolcanics (breccias, agglomerates, bedded tuffs and lavas) all inter-bedded with subordinate marine clastics, rare limestones, tuffaceous slates, re-deposited ash, and greywacke composed partly of volcanic fragments, exhibiting considerable lateral variations. The sequence, with a thickness reaching up to 2500 m in some sections, is metamorphosed to green schist facies except in contact aureoles of pluton (Asrat et al., 2003).

2.3 Structural setting of the region

The dominant strike of Precambrian faults is north-northeasterly. They form several major lineaments extending from 70 to 80km which are each composed of several faults and overthrusts. The most significant fault belt runs along the eastern and parts of western limbs of the Negash graben-syncline (Garland, 1980). The tectonic structure recorded by the Tsaliet and Tambien Group rocks is the result of stress during the amalgamation of island arcs to form ANS (Johnson et al., 2003).

Generally, two phases of deformation (D1 and D2) are recognized (Alene, 1998; Alene and Sacchi, 2000; Alene et al. 2006). Phase one deformation (D1) is caused by a N-S compression and resulted in tight minor folds with a wavelength of several mm to dm, elongation lineation and pervasive regional foliation (Alene et al. 2006). While phase two deformation (D2) resulted from an E-W directed compression at the waning stage of the collision between East and West Gondwana and yielded long wave length (about 8 km), upright, open parallel folds without a significant cleavage, thrust and strike slip faulting (Alene et al. 2006).

2.4 Geochemistry

The recognition of ophiolites and their dismembered fragments, together with the identification of chemically distinct island-arc volcanic and plutonic complexes in the Arabian–Nubian Shield, has led to general agreement that this part of the continental crust developed through horizontal crustal accretion during closure of the Mozambique Ocean. The presence of highly dismembered ophiolite suites which define suture zones that can be traced southward from the Arabian–Nubian Shield into the Mozambique Belt supports the idea that collision was the dominant orogenic mechanism throughout the East African Orogen (Timothy et al., 2003).

The Present widely accepted idea on the geotectonic crustal evolution of the ANS is that it has been developed by lateral crustal growth dominated by subduction-related processes and enigmatic arc construction through preponderate role of repeated plate boundary convergence, formation of intra-oceanic island arc system, subsequent ocean closure, amalgamation of the arc complexes and accretion to continental crust (Stern, 1994). Therefore, the arc terranes are believed to be intra-oceanic island arc/back arc-basin complexes (Stern, 1994).

Integrated studies including radiometric dating, isotopic and geochemical investigations, especially in the Arabian side of the shield (e.g. Roobol et al., 1983; Stoeser and Camp, 1985 as sited by Tadesse et al., 1999) have shown that the cratonization process involved a progressive change in chemistry of the arc magmatisim from early(> 900Ma.) primitive, low-K, arc tholeiite to late (700-600 Ma) evolved, high-K, calc-alkaline lava series.

Many authors (e.g. Alene et al., 1998; Asrat et al., 2001; Avigad et al., 2007; Kazmin, 1973; Miller et al., 2011; Tadesse et al., 1999, 2000; Teklay, 1997; Woldehaimanot, 2000) shows the Tsaliet Group of northern Ethiopia represents an arc volcanics sequence or subduction-related arc accretion of the ANS.

Records of a lower sequence of igneous rocks associated with arc magmatism in and around the southern ANS sector of the Mozambique Ocean is exemplified by calc-alkaline plutons and associated metavolcanic rocks of the Tsaliet Group. In western Tigre, the Tsaliet Group may be preserved as a series of accreted volcanic arc terranes within a suprasubduction setting (Tadesse et al., 2000). The Tsaliet Group is several kilometers thick and represents an arc volcano-sedimentary sequence (Teklay, 1997; Alene et al., 1998; Tadesse, 1998; Tadesse et al., 1999) or an arc–back–arc system (Teklay, 2006).

Mineral assemblages in the Tsaliet metavolcanics of East African Orogen in northern Ethiopia indicate that peak regional metamorphism at pumpellyite–actinolite to lower

greens schist facies (∼245–375◦C by chlorite thermometry) was attained coeval with

D1(Alene, 1998; Alene and Sacchi, 2000).

CHAPTER THREE

3. LOCAL GEOLOGY AND PETROGRAPHY

3.1 Introduction

The study area is a part of the Precambrian rocks of Tsaliet Group predominantly represented by metavolcanic and metavolcanclastic units. During the field work, record of outcop and lithologic data interms of color, texture, mineralogy, fabric, kind and degree of weathering and structural elements have been described. The size and shape of clasts also described. Except at few localities where the foliation of the rocks are weak and degree of weathering is high, the outcrop pattern follows the general structural trend of the area. These structural trends are mainly oriented NW and NE direction with dominantly moderate to subvertical SW and SE dippning. The ridge in the area also seen following similar direction with the regional trend.

During mapping, the MVC and MV units shows some intercalation making the contact relation to be variable. In between each units of MVC and MV gradational contact is dominant but it shows sharp contact when come to the boundaries between MVC and MV. In general, six mappable units are encountered. The geology of the study area is shown on the map (Figure 3.11). All mappable units in the study area are divided and described as follows:

- ✓ Metavolcanic (MV)
    - Metabasaltic andesite and meta-andesitic
- ✓ Metavolcanoclastics (MVC)
    - Metabreccia,
    - Tuffaceous layer
    - Slate

- ✓ Phanerozoic sandstone
- ✓ Phyllite and slate are rocks found as intercalation between the metavolcanic and metabreccia units.

3.2 Metavolcanic units

From field observation and additional petrographic studies of thin section two types of intermidiate metavolcanic units have been identified.

3.2.1 Meta-andesitic

Meta-andesitic unit exposed extensivelly in the eastern part the study area with considerable thickness compared to other units. It forms moderate to gentle topography and the nature the exposure is massive, affected by joint and fracture and slightly foliated (Figure 3.1 A & B). It is characteristically light green, grey to dark grey with white shiny surface possibly due to the presence of quartz and plagioclase with weathered brownish color. It has fine to medium grained texture at hand specimen level and in thin section. Locally, it shows intercaletion with the slate units. Unlike other units, this unit is not/least affected by quartz vein. It shows weak foliation generally trending NE - N15^{0}E with some NW strike dipping subvertically to the southeast. The contact it makes with adjecnt units is more of gradational type contact and sharp contact is observed when it is found intercaleted with other units.

Figure 3.1 Field photograph of meta-andesitic units. A) outcrop of meta-andesitic unit southeast of the study area (578976E, 1532479N, photo taken facing west) B) meta-andesitic unit from central east part of mapped area (578943 E, 1532618N, photo taken facing east).

Thin section

Thin section from this unit shows quartz, chlorite, muscovite/sericite, epidote, altered plagioclase/albite, calcite and opaque minerals. In addition, significant amount of feldspar and trace amount of actinolite/tremolite, relict olivine and pyroxine are observed (Figure 3.2 A - D).

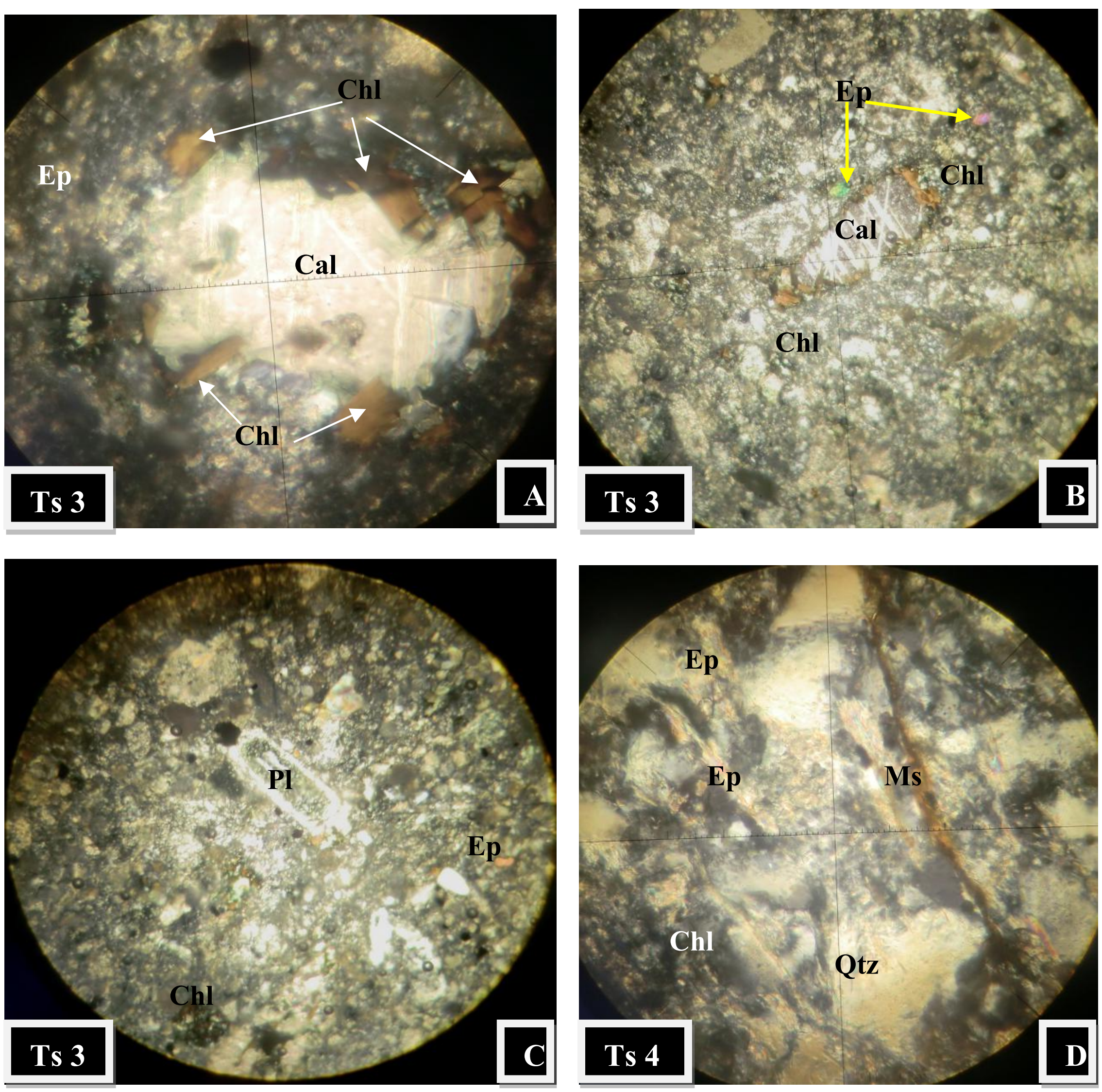

Figure 3.2 Thin section photographs of meta-andesitic units. A) secondary minerals of chlorite and calcite replacement in meta-andesite B) randomly oriented calcite and chlorite mineral C) alteration of plagioclase into sericite minerals D) recrystallized quartz epidote, chlorite and muscovite minerals from other thin section of meta-andesitic units. Plate A, B & C are XPL pictures, with 10x10 total magnification except 40x10 magnification for plate A. Location (578962E, 1534190N). Plate D is in XPL view with 10x10 total magnification. Location (578885E, 1532565N).

From plate A, B & C mineral content: 30-35% quartz, 15-20 % sericite, 10% calcite, 10% chlorite, 2-3% muscovite, 2% opaque, 2 % epidote and minor constituents of relict olivine/pyroxene and plagioclase. The quartz grains are recrystallized and deformed exhibiting undulose extinction. They have rounded to angular shape. The plagioclase show alteration to sericite. All specimen shows weak foliation however, S1 foliation is rarely observed by the alignment of quartz, altered plagioclase and sericite. In plate A chlorite is replaced by calcite and they appear to be randomly oriented with the pre-existing foliation and are probably post-tectonics to D1 (Figure 3.2 A, B & C).

Plate D mineral content: 30% quartz, 15% muscovite, 15% chlorite, 10% sericite, 10% calcite, 5% plagioclase/albite, 5% epidote, 2% opaque and trace amount of relict olivine/pyroxene. The specimen shows weak foliation but S1 foliation is observed marked by mica and sericite wrap around angular to sub rounded quartz (Figure 3.2 D). Certain minerals like quartz are enclosed in the bigger porphyryoblast giving the host crystal a spongy appearance poikiloblastic structure, or sometimes termed as sieve structure from the same specimen (Figure 5.2 A). The microlithons in plate D are not crenulated hence the foliation can be called disjunctive foliation (Figure 3.2 plate D).

Based on the mineral composition and minor schistosity under microscope, the rock has been named as epidote-mica-chlorite-sericite-quartz schist.

3.2.2 Metabasaltic andesite unit

This unit is characterized by having dark green color mineral, elongate green shiny mineral possibly actinolite/tremolite and medium to course grained texture at hand specimen. It is found in the western part of mapped area dipping to the west and also found in the east part dipping to the east. The dip of this unit is moderate in the eastern part but shows sub vertical dipping in the western part of the study area. It shows weak foliation striking NE to 340^0. It forms somewhat moderate to gentle topography and the nature of the exposure is massive and affected by joint.

Thin section

Two thin section from this unit is prepared and examined under microscope. The rock dominantly consists of epidote, chlorite, amphibole, calcite, altered plagioclase/albite, actinolite/tremolite and quartz minerals. Other minerals like, muscovite, olivine, pyroxine and trace amount of opaque possibly rutile/manganise? and altered sericite are present (Figure 3.3 A-D).

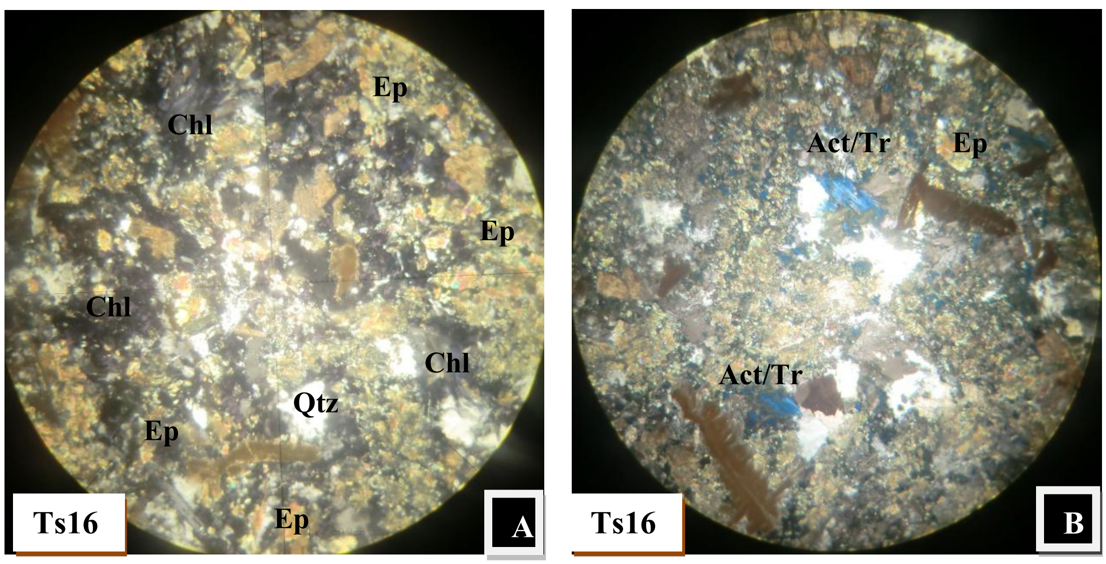

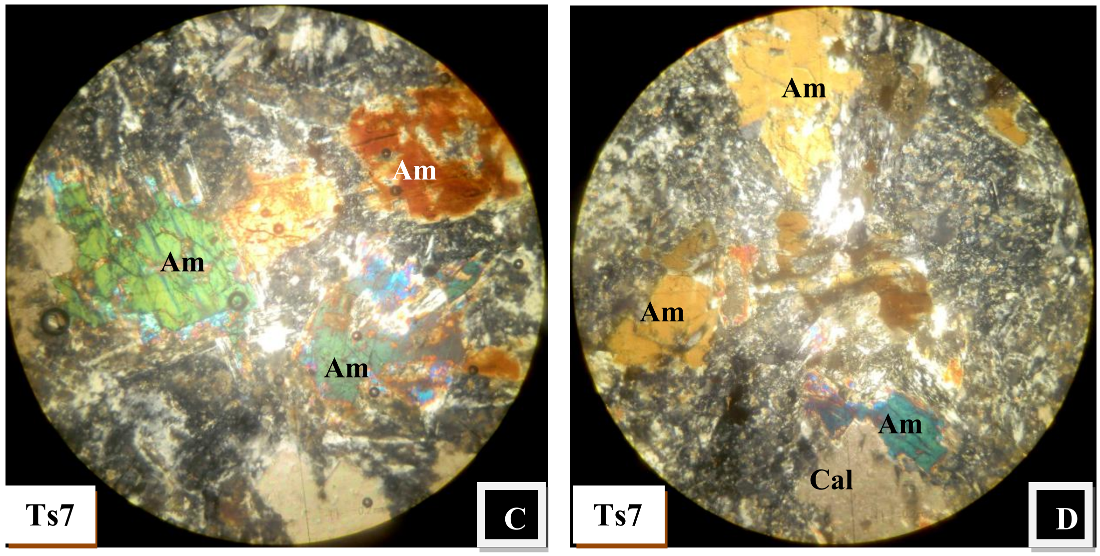

Figure 3.3 Thin section photographs of metabasaltic andesite showing alteration and replacement A) epidote mineral showing epidotization in metabasaltic andesite B) randomly oriented actinolite/tremolite mineral C) & D) replacement of mafic mineral like amphibole by secondary minerals of calcite and quartz. All view under XPL with total magnification of 10x10. Location (Plate A & B: 574608E, 1531446N; plate C & D: 577910E, 1533719N).

From plate A and B: the average modal composition from thin section (Ts16) Figure 3.3 A & B showed that 30-35% epidote, 20-25% chlorite, 10% calcite, 10% quartz, 5% actinolite/tremolite, 5% alkali feldspar, 5% relict plagioclase and 3% opaque. It shows weak foliation and most of the crystals are randomly oriented. Epidotization and sericitization are the main alterateration process in this units under thin section (Figure 3.3 A & B). Silicification is the other alteration process that is responsible for the formation of polycrystalline quartz grains. Recrystallized angular to sub rounded quartz grain shows undulose extinction that are features of pretectonic structure. Minerals like actinolite/tremolite, chlorite and mica shows random orientation giving decussate texture. Based on the mineral assemblages the metamorphic name gives as plagioclase- quartz-chlorite-epidote- schist.

Plate C and D: the average modal composition from thin section (Ts7) (Figure 3.3 C & D) showed that 15-20% amphibole, 10-15% chlorite, 10-15 quartz, 10% calcite, 5-10% feldspar (microcline), 5-10% actinolite/tremolite, 5% epidote, 5% altered plagioclase, 5% muscovite, 3-5% olivine/pyroxine and 2% opaque. The quartz grains are recrystallized mostely replacing plagioclase found as polycrystalline quartz grain due to deformation. They have rounded to angular shape exhibiting undulose extinction. Minerals like biotite, muscovite, quartz and feldspar are active minerals in alteration. The feldspar plagioclase show alteration to calcite and sericite with remnant albite twinning left. Broken, fractured or boundinage crystal of quartz is common indicating pretectonic structure. Certain minerals like quartz, mica and opaque are enclosed in the bigger porphyryoblast of biotite and hornblende (Figure 3.3 plate C & D) giving a spongy appearance poikiloblastic structure or sieve structure.

Based on the mineral assemblages the metamorphic name gives as feldspar-quartz-chlorite-amphibole schist.

3.3 Metavolcaniclastics

3.3.1 Metabreccia

This units is the dominant lithologic unit occurring extensively in the western part of the study area. It is characterized by forming hill in the NW part and somewhat gentle topography in the SW part of the study area. The exposure is continuous and blocky affected by quartz vein. The color of the outcrop shows dark black and grayish weathered color but the fresh sample show variation in color depending on the amount, type and size of the clasts and fragment (Figure 3.4 A & B). The size of the clasts ranges from 2 - 15 cm most of them are sub rounded to sub angular in shape. There are also large clasts and fragments that range in size from 10 - 60 cm in diameter and most of them are characterized by sub rounded to angular in shape. The metabreccia unit show sharp contact with the adjacent meta-andesitic units. In addition, it is rarely found intercalated with the other units but occur between other rocks which is not insitu. It shows general trend N- S to 330^0 but locally it shows $N15^0E$ to 330^0 direction with 65^0 to 80^0 dip towards SW.

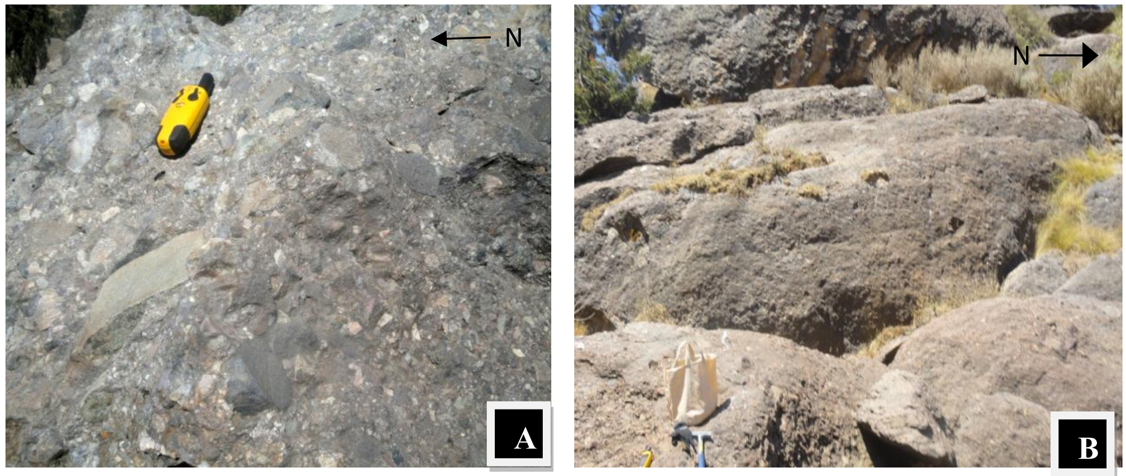

Figure 3.4 Out crop of metabreccia A). outcrop of Metabreccia unit from southwest part of mapped area (574146E, 1531253N, photo taken facing east) B). outcrop of metabreccia unit from northwest part of mapped area (574462E, 1535889N, photo taken facing west)

Thin section

This unit mainly of composed quartz, plagioclase, sericite, calcite and some mafic minerals together with few rock fragments. It shows weakly developed schistosity and the fragments are being wrapped by the mica minerals. Most of the minerals show random distribution (Figure 3.5 A-D).

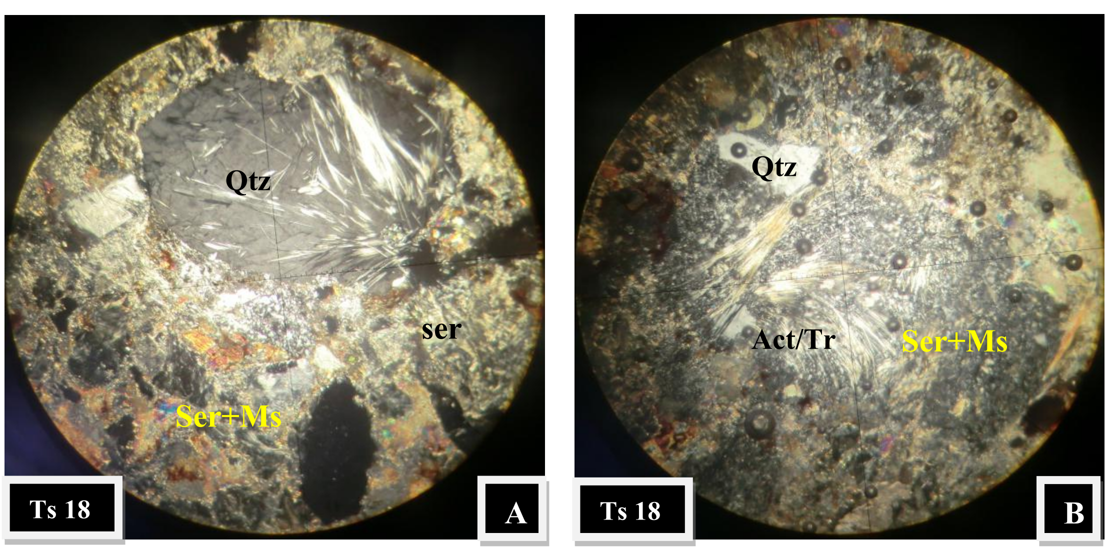

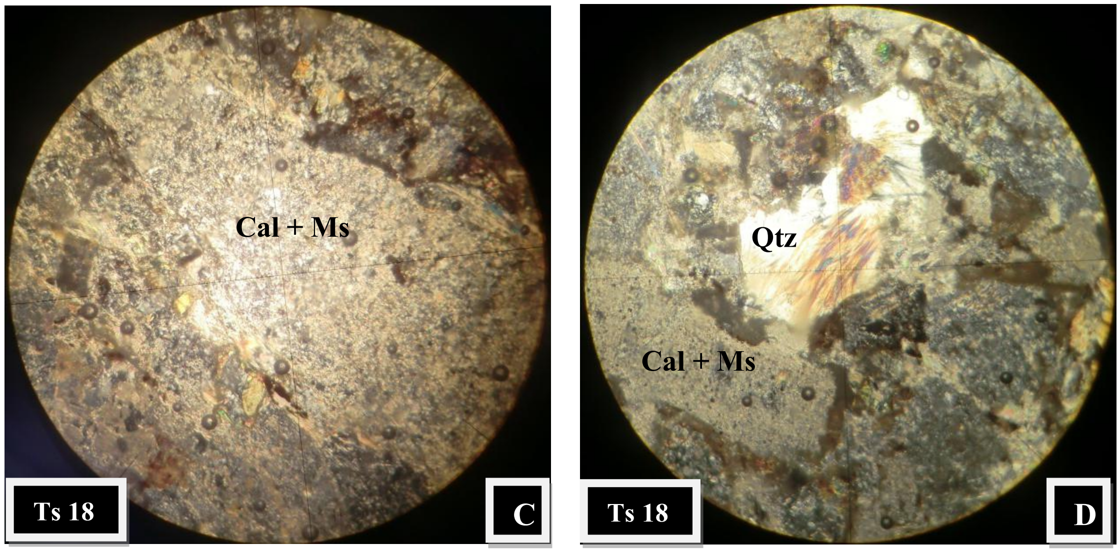

Figure 3.5 Microphotographs of metabreccia. A) quartz with radiating fibers along with sericite and muscovite B) fine grained muscovite and sericite matrix C) elongated altered calcite and muscovite vein along the main foliation D) Quartz grains with radiating fiber. All under XPL view, total magnification 10x10 for all thin-sections. Location (574209E, 1531160N)

From plate A-D: The average modal composition from thin section (Ts18) (Figure 3.5) exhibit 20% quartz, 15% sericite, 12% muscovite, 10% calcite, 8% epidote, 10% opaque, 5% actinolite/tremolite, 5% plagioclase, 5% clasts and opaque minerals. Undulose extinction and diverging/branching needles in quartz and calcite are the prominant feature. Recrystallized anhedral to subhedral quartz grains show sutured boundary and undulose extinction due to later deformation. In addition to this, xenoblastic calcite, large sericite grains, broken feldspar (plagioclase), and minor randomly oriented biotite porphyroblasts are also present.

The presence of altered and fragmented plagioclase, devitrified volcanic glass, coarse calcite and quartz developed decussate structure. The presence of primary igneous origin minerals (plagioclase) volcanic glass and close association to the metavolcanic units indicates a pyroclastic origin of the unit.

These mineral assemblages gives the metamorphic name as plagioclase-epidote-muscovite-sericite-quartz schist.

3.3.2 Tuffaceous layer

The outcrop is often found as light yellow, brownish to reddish and black weathered color. At hand specimen when it is broken tiny elongated crystals of quartz and dark to grayish minerals are observed. The most observed characteristics of this units is the presence of vesicles and layering of white, gray and yellowish weathered surface (Figure 3.6 A and B). The rock also found strongly weathered (oxidized) as a result it is hardly possible to find fresh outcrop on surface. The nature of exposure is continuous, homogeneous and fragmental forming hill topography affected by at least three sets of joint.

The unit depicts some variation in color and composition of bedding across strike, it shows weathered dark grey color when it contacts with slate units to the east but dark brownish color when it contact the metagreywacke to the west of mapped area. Lithostratigraphically it shows gradational contact with slate units to the east and to the west of the mapped area. Structurally complex relative to the other unit which is affected by different sets of joints, strong foliation, different types of folding and veins are also observed. Some of this structure are superimposed on original layering of this unit.

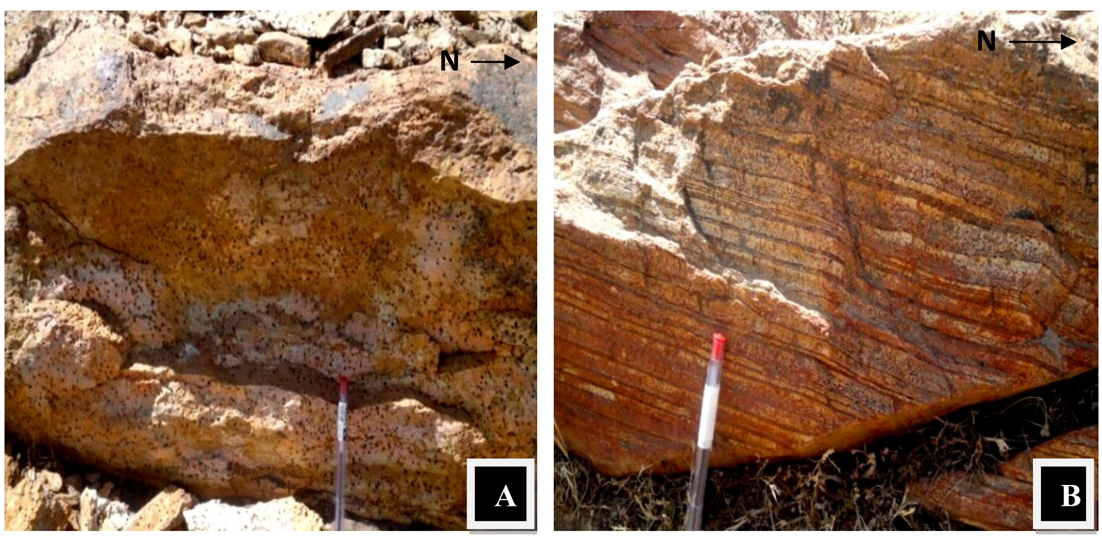

Figure 3.6 Tuffaceous layer A) outcrop of tuffaceous layer south west of the study area (574972E, 1533740N, photo taken facing west) B) tuffaceous layer from central east of mapped area (576957E, 1534693N, photo taken facing west).

The thin section from this units reveals that ~30-35% mica, ~20-25% sericite, ~10-15% quartz, ~5-10% relict calcite, 10% lithics, 5% opaque and ~2-5% volcanic glass.

3.3.3 Slate

This unit is fine grained and well laminated appear as variegated colors including dark grey, grey-green, pinkish and whitish color with steeply inclined foliations. It forms gentle topography relativelly to other units. The nature of exposure is fragmental, shows intercalation with the other units and moderatly foliated (Figure 3.7 A & B). It shows regional foliation trending N-S to 350^0 dipping moderate to sub vertical to the west and to the east. At places, the rock is affected by closely spaced joints and quartz veins. It shows sharp contact relationship with the adjacent metavolcanic units but gradational contact with the tuffaceous layer. The field observation at an outcrop and hand specimen level, shows greenish mineral alteration but also shows quartz, darkgreen shiney mineral and elongated white shiny mineral with some clasts.

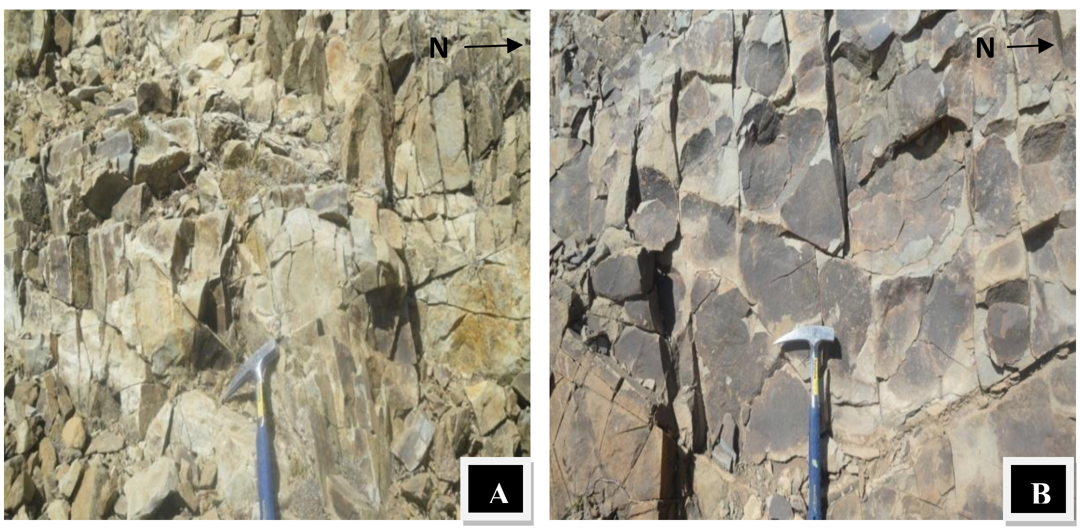

Figure 3.7 Outcrop of slate A) slate unit from south west of the study area (576972E, 1533740N, photo taken facing west) B) slate unit from central east of mapped area (576957E, 1534693N, photo taken facing west)

Thin section

The major minerals in this unit are quartz and sericite. The thin section analysis shows the presence of mafic metamorphic minerals (epidote and chlorite) that indicate the slate has a volcanic or volcanoclastic origin at present scale of observation. This unit mainly composed of crystal fragments of quartz, feldspar and sericite with small amount of epidote and chlorite. The grains are fine grained with some medium grained subhedral quartz crystals and weak foliation is observed. (Figure 3.8 A - D).

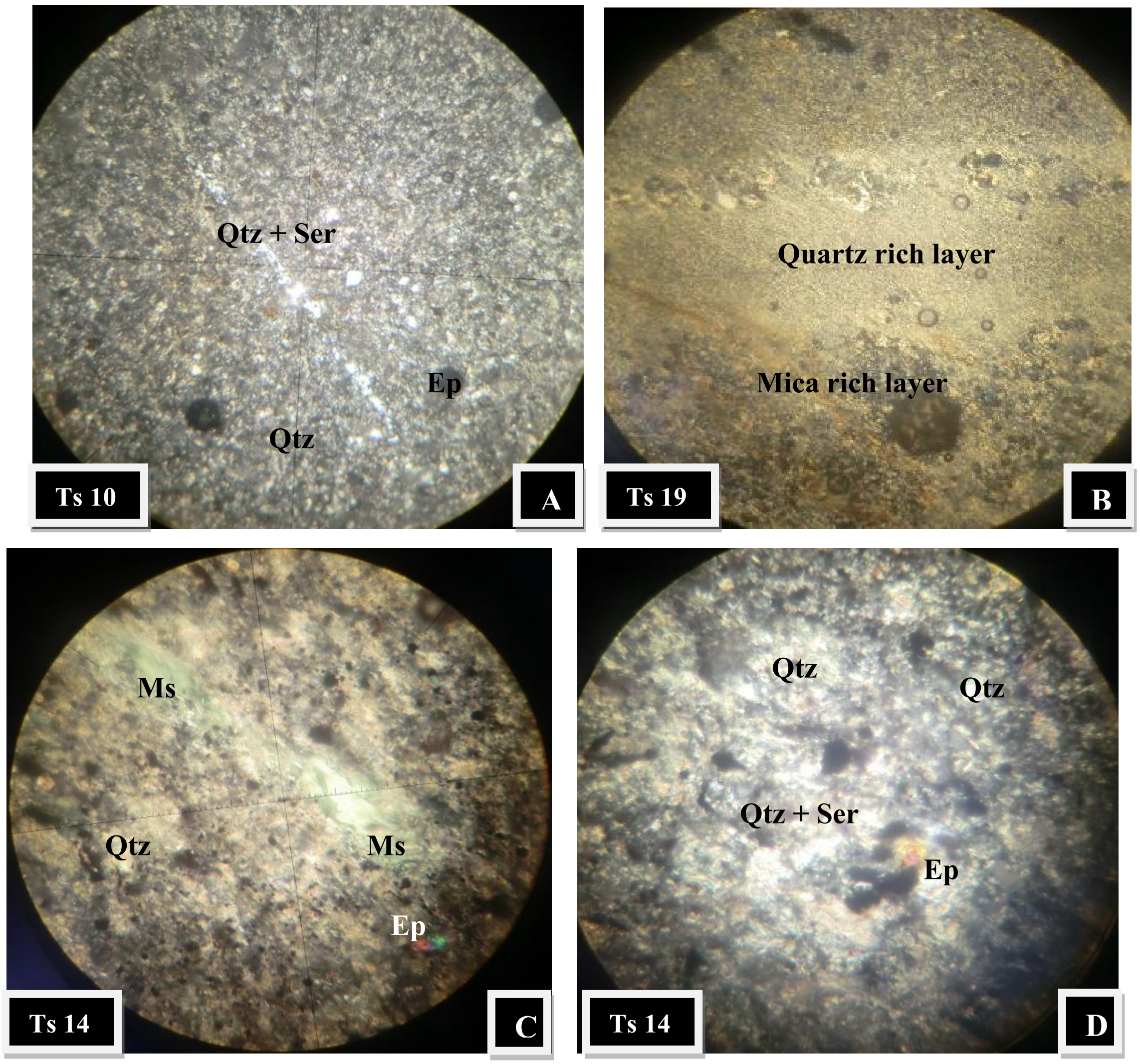

Figure 3.8 Microphotographs of slate. A) fine grained quartz and sericite showing weakly developed foliation S1 and thin quartz vein cross cut S1 foliation B) foliation defined by compositional layering in slate. The quartz rich layer is fine grained relative to the mica rich layer C) muscovite mineral along weakly developed foliation in fine matrix D) quartz, sericite and epidote minerals. All under XPL view. Plate A (576957E, 1534693N). Plate B (5757295E, 1533905N) with 10x10 total magnification for A & B. Plate C & D (574719E, 1531428N) with 40x10 total magnification.

The petrography of thin section from the slate (Figure 3.8 A & B) shows that 35-40% quartz, 25-30% sericite, 5-10% muscovite, 6% altered biotite, 6% opaque, 3% epidote, 1% chlorite and trace amount of altered feldspar (plagioclase) and calcite. Some quartz crystal shows random orientation with the weakly developed S1 foliation. Quartz veins cross cut the S1 foliaton (Figure 3.8 B). The sericite are observed as a fine grained ground mass and some with medium texture mostly altered product of feldspar and quartz (Figure 3.8 A).

Other thin section from this units (Figure 3.8 C & D) shows that 35% of sericite, 20% quartz, 10% muscovite, 10% opaque, 5% calcite, 3% fine grained chlorite, 5% volcanic glass, 2% epidote. Most of the mineral show well devloped foliation.

These mineral assemblages give the metamorphic name as epidote-chlorite-muscovite-quartz -sericite schist.

3.4 Phanerozoic sandstone

The Phanerozoic sandstone is exposed on the central east part of the study area between the metavolcanic units. These rocks show angular unconformity with metabreccia units in the western part of the study area but the contact to the metavolcanic around the main road from Atsbi to Wikro is somewhat difficult trace. In the study area the Phanerozoic sandstone rock shows some color variation. The light yellow, gray to whitish sandstone characterized by medium grained, well sorted, highly friable and dominated by quartz with large clasts. This unit is regionally correlated with Enticho sandstone (Beyth 1972). This units shows clear cross-bedding structure (Figure 3.9 A & B). The other type is somewhat shows reddish to dark brownish, medium to course grained found in the contact zone with the adjacent metavolcanic units.

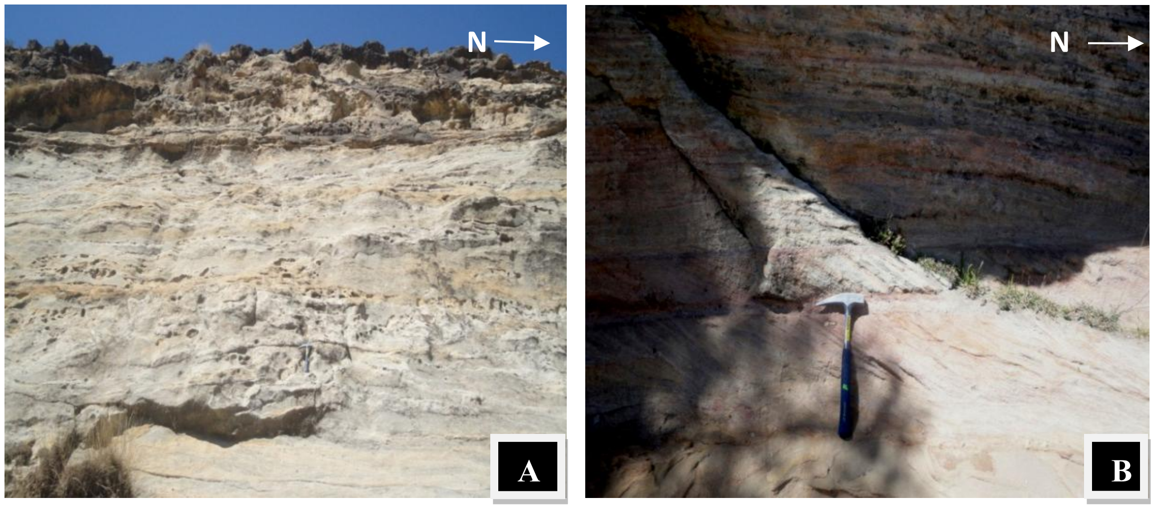

Figure 3.9 Phanerozoic sandstone A). phanerozoic sandstone east of the study area (578486E, 1532660N, photo taken facing west) B). phanerozoic sandstone east of mapped area (578273 E, 1532681N, photo taken facing west)

3.5 Quartz vein

During the the course of mapping, description and sampling of quartz veins with their areal extent, attitude and contact relation also studied. Three generations of quartz veins occur in the study area cutting and/or parallel to S1 foliation. The first generation quartz veins are folded by D2 and less abundant as compared to the unfolded second and thrid generations. The second generations are those that runs parallel to the regional foliation. The third generation of quartz veins are found associated with joints and fractures and crosscut the regional trend (Figure 3.10 C). They represent the younger veins relative to the second generation which are not affected by S1 foliation. The quartz vein in metabreccia units are large, continuous having a size range from 10 - 50 cm thickness but partly covered by the trees and also scattered on the ground (Figure 3.10 A). Others veins have a width ranges from 1 to 5 cm. All shows different attitude NW, SW sometimes EW trend (Figure 3.10 B & C).

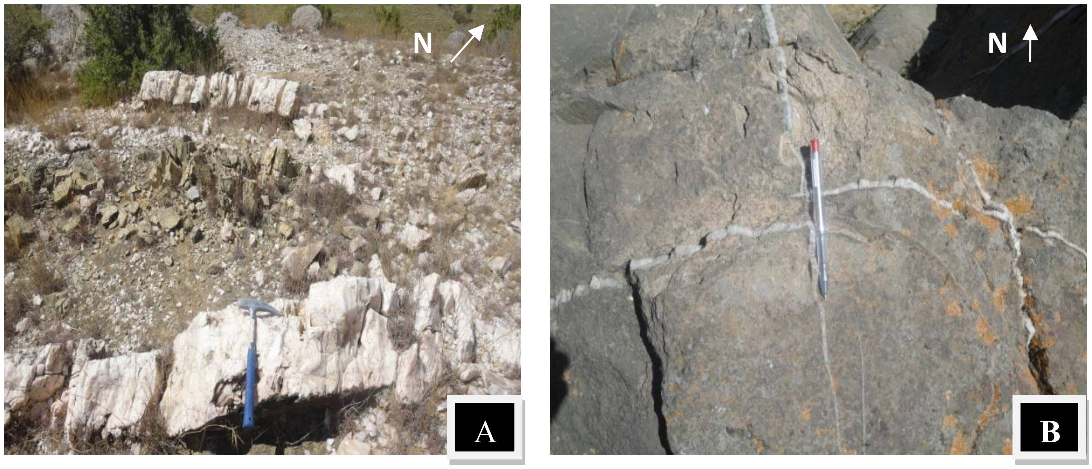

Fig.3.10 Field photographs showing quartz veins (A) quartz vein at the outcrop of metabreccia unit from southwest part of mapped area (0574146E, 1531253 N, photo taken facing east). (B) & C) quartz vein found within weathered metavolcanic rocks photo taken facing north and west respectively.

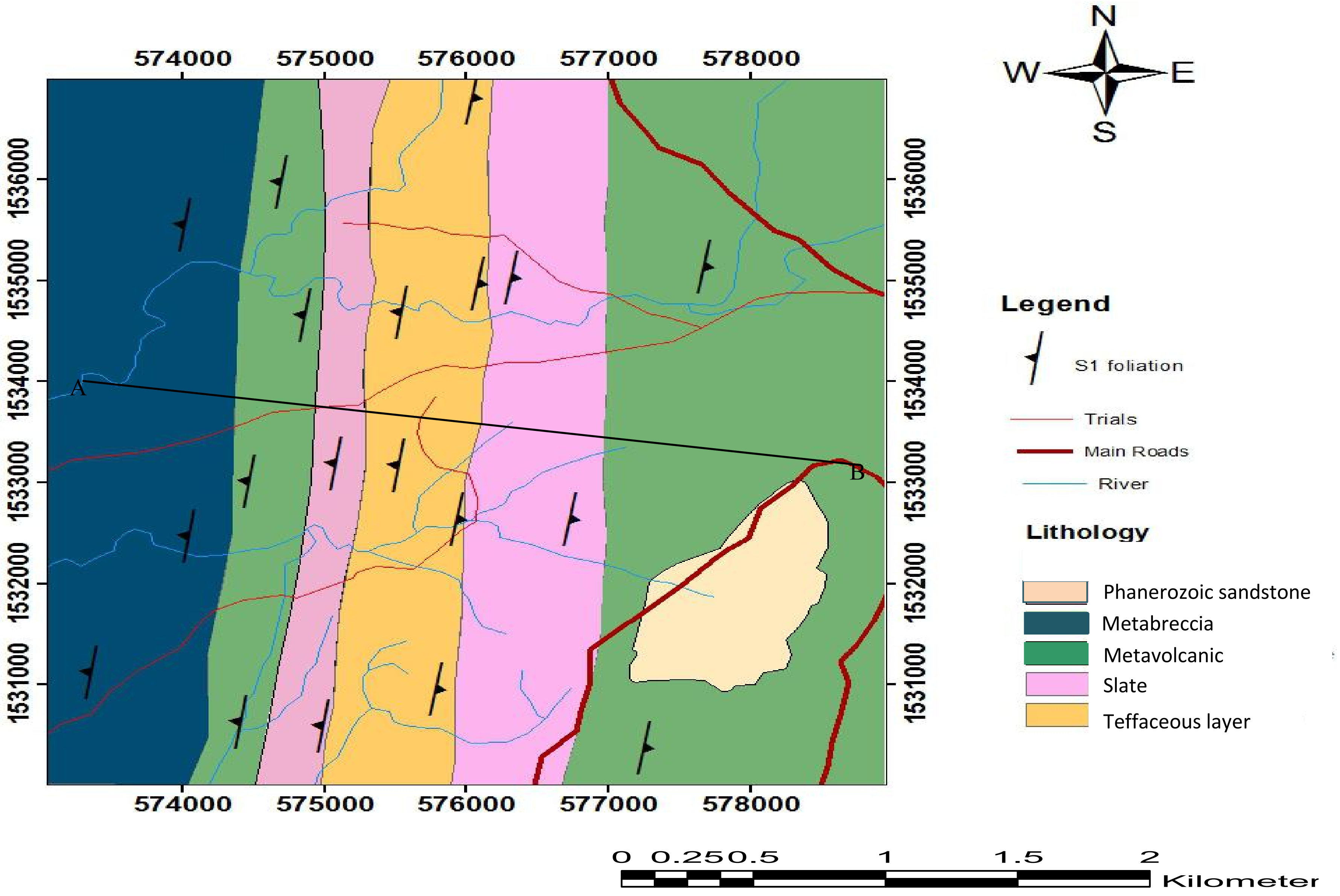
N
W
E
S
574000
575000
576000
577000
578000
1536000
1535000
1534000
1533000
1532000
1531000
A
B
Legend
S1 foliation
Trials
Main Roads
River
Lithology
Phanerozoic sandstone
Metabreccia
Metavolcanic
Slate
Teffaceous layer
0
0.25
0.5
1
1.5
2
Kilometer

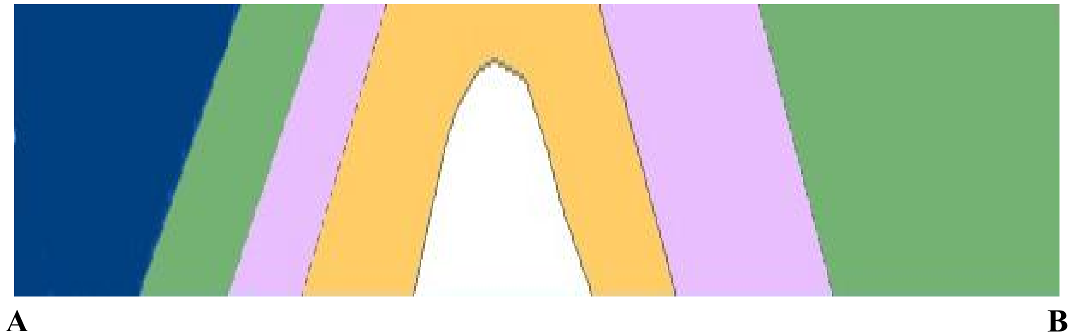

Figure 3.11 Local map and cross section of the study area.

CHAPTER FOUR

4. DEFORMATION AND STRUCTURE

4.1 Introduction

All field measurement and thin section study of structures, deformation and microstructural analysis have shown that the Precambrian rocks of Atsbi area have been subjected to polyphase deformation. This polyphase deformations is marked by the existence of different types of structural elements such as regional pervasive foliation, multiple folds and lineations, as well as various sets of joints in rocks of the study area. In general, the mapped area experienced two phases of ductile deformation (D1 and D2) and a later phase of brittle deformation (D3).

4.2 D1 Deformation and associated structures

The rocks that were deformed and metamorphosed during earlier deformational phase (D1) due to N-S compression and related to the collision of East and West Gondwanaland (Alene et al., 2006) resulted in the development of sub-vertical tight folds, moderate to strongly developed sub-vertical S1 foliation. The S1 foliation is sub parallel to the initial lithological layer (S0) in the tuffaceous layer and slate unit that preserve original layering/bedding.

4.2.1. F1 Folds

Related to D1 phase, the types of folds occur in the study area are not as common as the folds that characterize D2 phases. These folds are found mainly in tuffaceous layer and in some metavolcanic units as folded quartz vein showing 55^0-70^0 plunging folds and subvertical to vertical folds in quartz vein (Figure 4.1). The orientation of the fold is compatible with N-S oriented D1 shortening. Regionally this type of folds are associated with D1 deformation (Alene et al., 2006).

Figure 4.1 Sub vertically folded quartz vein plunging 80^0 towards 20^0 with A.P 030/67SE. Location (578639E, 1531560N; photo taken facing East).

4.2.2. S_1-Foliation

S1 foliation is prominent throughout the study area but more developed in slates and tuffaceous layers (Figure 4.2 A & B). Although it shows some variation locally, the foliation shows general trend of 340^0 - 020^0 dipping 45^0 - 85^0 SW or/and SE. It is usually sub-parallel to the initial lithological layering (S0). Bedding commonly encountered in tuffaceous layer (Figure 3.6) and slate units. The beds have various color and thickness that range from 1cm to 15 cm. The bedding majorly consists grayish, brownish and dark gray to dark layer. Microscopic examination of thin section from slate units shows compositional layering characterized by quartz and mica rich layers that are considered to represent S_0/primary lithological layering (Figure 3.8 B).

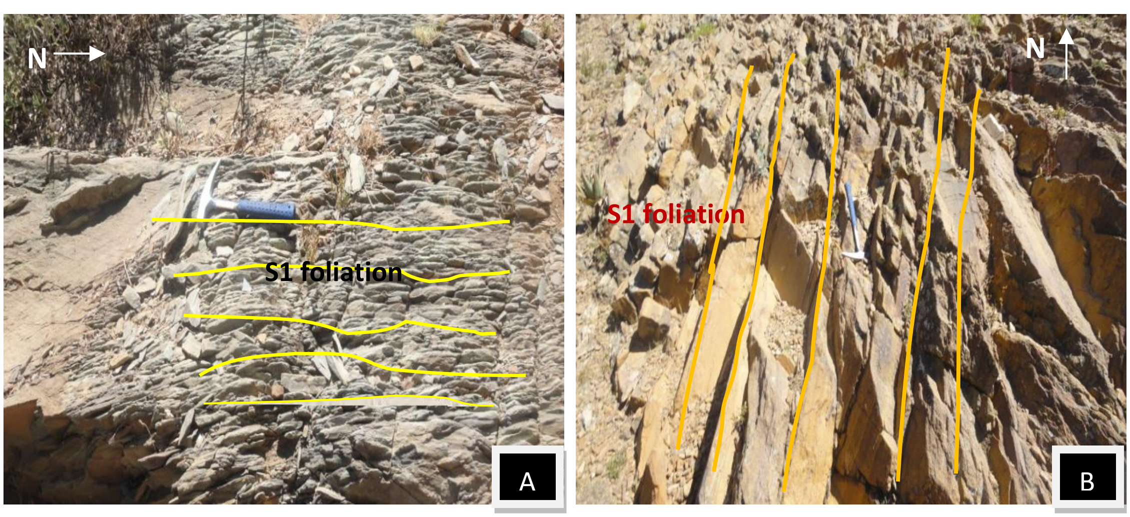

Figure 4.2 A) S_1 foliation in Slate (578976E, 1532479N; photo taken facing west) B) S_1 foliation in tuffaceous layer (575733E, 1531617N; photo taken facing north).

4.2.3. L1 Lineation

This structural elements are observed in metabreccia and in some metavolcanic units showing moderate to sub vertical plunging, generally 50^0 - 70^0 mostly north east. The elongated and stretched pebbles/clasts have been observed in the rocks displaying elongation and stretching lineation in the field mainly in metabreccia unit (Figure 4.3A). The shape and orientations of the stretching and elongated pebbles and clasts shows sub-parallel to the S1 regional foliation that could be correlated with D1 deformation. The other L1 lineation type in the study area is the intersection lineation that shows the intersection of Bedding (S_0) and S_1 foliation (Figure 4.3B).

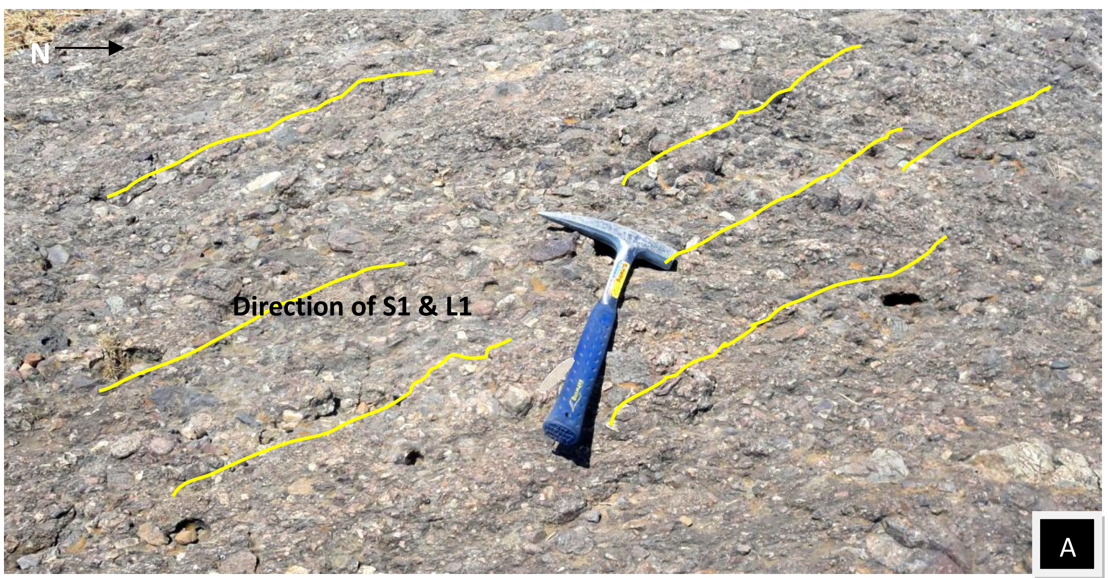

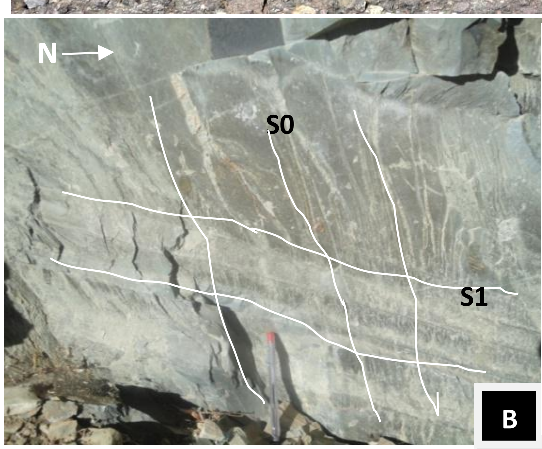

Figure 4.3 L1 lineation A) elongated and stretched pebbles/clasts displaying elongation and stretching lineation in metabreccia units (574462E, 1535889N; photo taken facing west). B) intersection lineation between bedding and S1 foliation in meta-andesitic units (Location (578984E, 1533645N; photo taken facing west)

4.3. D2 Deformation and Associated Structures

Prominant large scale feature as well as mesoscopic to microscopic structure associated with the second phase deformation are well developed in the map area. Mesoscopic folds formed during D2 are generally open, upright and hamonic that mostly plunge south.

4.3.1. F2 folds

The F2 folds are well exposed in the study area that are characterized by open and upright harmonic folds (Figure 4.4 A - F and 4.5) mostly shallowly plunging south. They are observed largely in tuffaceous layer, in metabreccia and also metavolcanic units (as maifested by folded quartz veins). Quartz veins mostly appear as fracture filling and locally shows cross cutting relationship. They are predominantly associated with joint and fracture but these veins once fill the fracture, they may be folded by D2 and resulted open shalow plunging folds associated with the host rock (Figure 4.4 E & F).

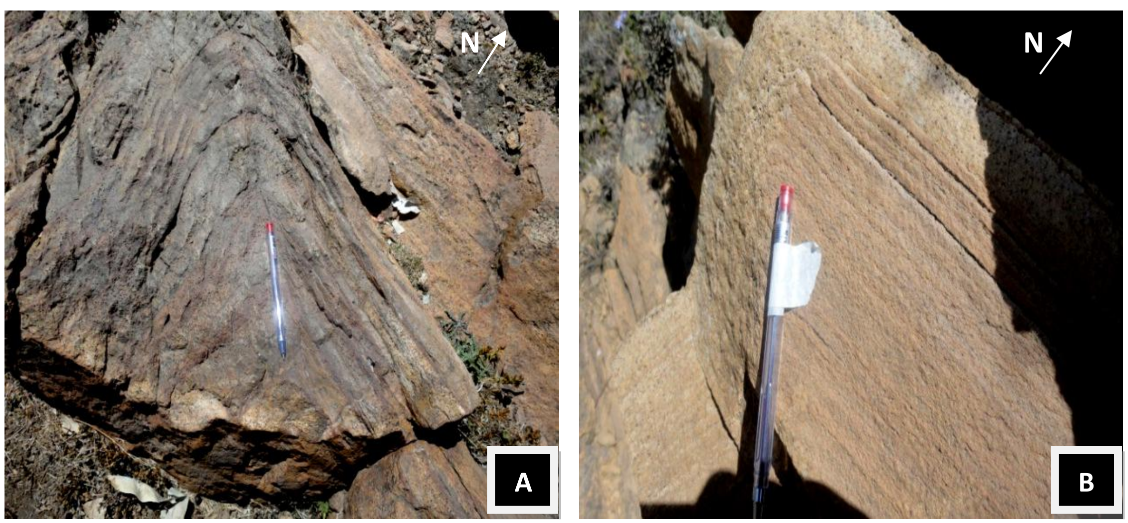

Figure 4.4 Field photos of mesoscopic folds with horizontal to sub horizontal fold axes. A) upright harmonic fold within tuffaceous layer plunging 20^0 towards 185^0 with A.P 190/65SE (575820E, 1533747N; photo taken facing south west) B) open harmonic fold plunging 20^0 towards 160^0 with A.P 150/55SW in tuffaceous layer (575773E, 1532733N; photo taking facing south west) C) upright fold with gently 12^0 towards 178^0 with A.P 180/30W in tuffaceous layer (575312E, 1533702N; photo taken facing south west) D) folds with open moderate plunging fold axis manifested by quartz vein in metabreccia units plunging 45^0 towards 050^0 with A.P 030/70SE (574265E, 1534297N; photo taken facing north east); (E & F) folded quartz vein in metavocanic units (576496E, 1530581N; photo taken facing south).

A fold with a fold axis plunging 15º towards 165^0 has been observed in tuffaceous layers characteristically a poly harmonic upright fold (Figure 4.5).

Figure 4.5 Polyharmonic upright folds plunging 15^0 towards 165^0 with Axial plane 210/45NW (575852E, 1533758N, photo taken facing SSW)

4.3.2 L2 Lineation

L2 lineation in the study area is the one defined by the relation with F2 fold axes. These lineations have similar orientation with the fold axes of mesoscopic open and upright folds of the area defined by the F2 fold axes and related intersection lineation. That could imply they are probably of the same generations. Most are shallow plunging, 14^0 - 25° → SW. The stereo plots of F2 fold axes and lineation show a cluster of points either very close to the primitive circle or on the primitive circle of the net in southern poles that indicates shallow plunging mostly south west (see Figure 4.9).

4.4. D3 phases and associated structures

Conjugate brittle structures like joint and fractures almost affect all litho units in the study area. Joint with many sets of joint system that are superimposed at shallow and high angle to the D1 and D2 structure characterize D3 phase of deformation.

4.4.1 Joints

Joints are the other dominant structure in the study area that occur in various form and divide into four sets of joints with NW, SW, NE and to some extent SE joints trending moderate to sub vertical dipping. These conjugate brittle structure affect predominantly the slate, metavolcanic (Figure 4.6 A & B) and tuffaceous layer with atleast four sets of joint mostly at high angle to the D1 and D2 structures. They crosscut the regional foliation and characterize D3 deformation representing the younger deformation phase. Locally they shows cross cutting relationship indicating the presence of polyphase deformation marked by the variation in occurence and distribution of those joints in each units. Generally they show 30 cm to1m joint spacing but some others are even closer to each other with 10 to 15cm.

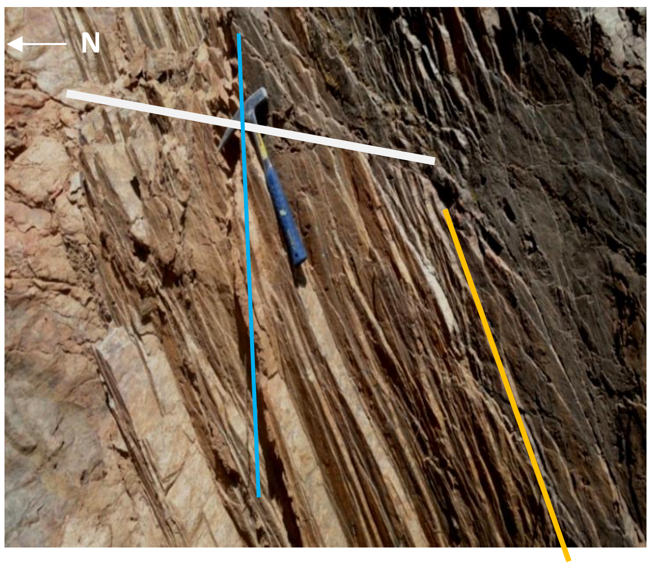

Figure 4.6 A) three sets of joint that cut the weathered metavolcanic units (577210E, 1530610N; photo taken facing east)

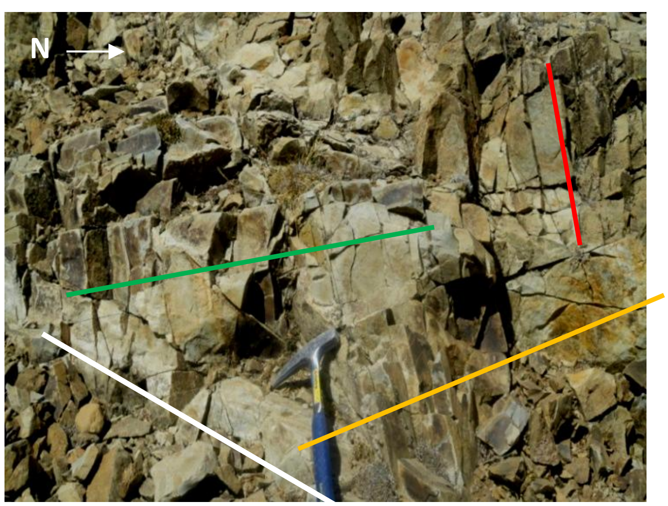

Figure 4.6 B) four sets of joint showing different orientation that cut through the slate units (576957E, 1534693N; photo taken while facing west)

4.5. Equal area projection of different structure

Equal area projection allows analysis of structure in situation where the structures are very large scale or are not well exposed and data form isolated outcrop may be combined to characterize the fold geometry. The equal area plots for all S1 foliation (Figure 4.7 A & B) shows that the poles are not in random orientation but shows structural trend. These poles are clustered in the SE and NW quadrants of the net and the mean girdle of the poles indicates a plunging fold (15^0 towards 192^0). On the other hand the plots of poles for joint (Figure 4.10 A & B) shows different sets of orientation due to the existence of different sets of joint that cuts the S1 foliation and this brittle structure represent D3 deformation phases.

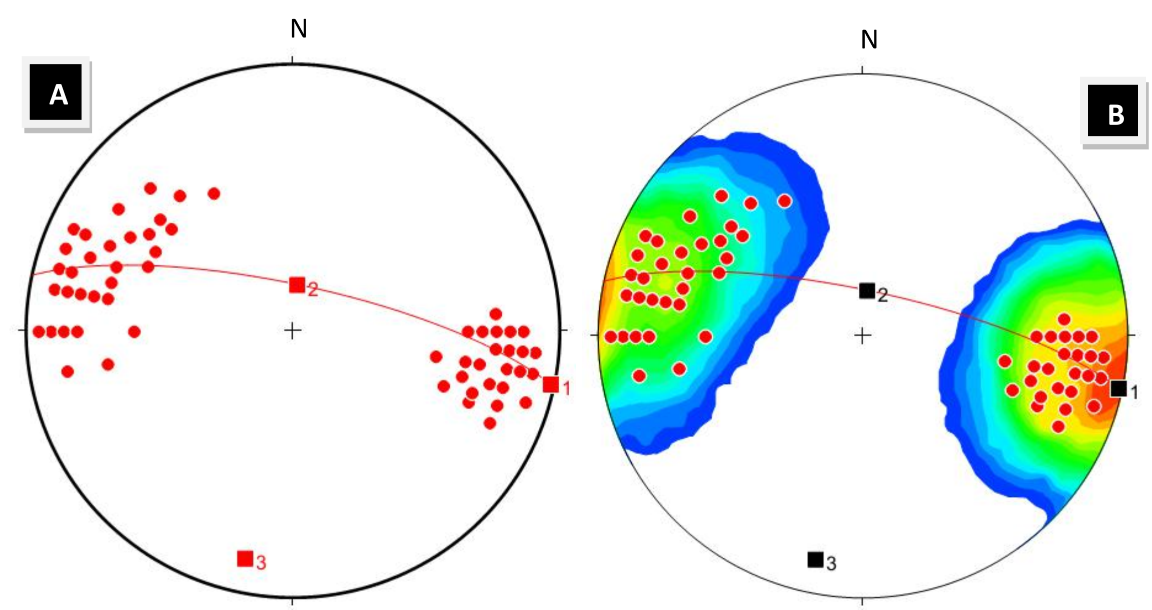

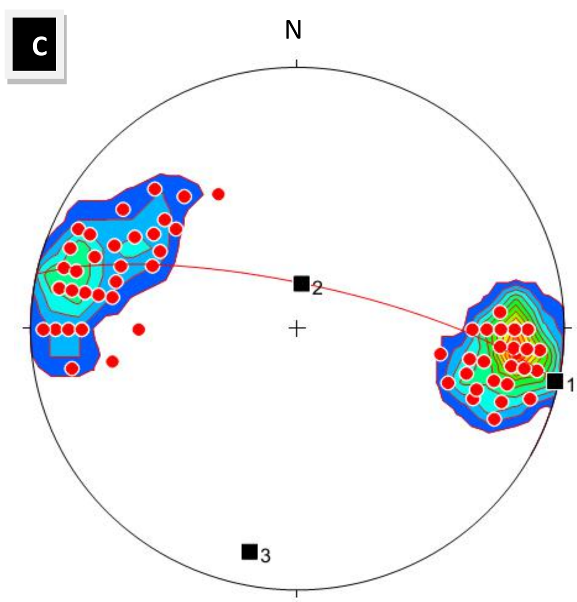

B. Kamb Contouring method

- Contour Int. = 2 sigma;
- Counting Area = 11.1% of net area
- Signif. Level = 3 sigma
- counting grid spacing (x and y) =30

C. 1% area contouring

- Contour Int. = 2%;
- Counting area 1% of the net
- Counting grid spacing (x and y)

Figure 4.7 A) Equal area plots of S1 foliation as the poles calculated from72 planes. B) contours of poles in Kamb methods showing gridded density of the prominent foliations (S1) C) 1% area contouring method showing cluster poles of S1foliation.

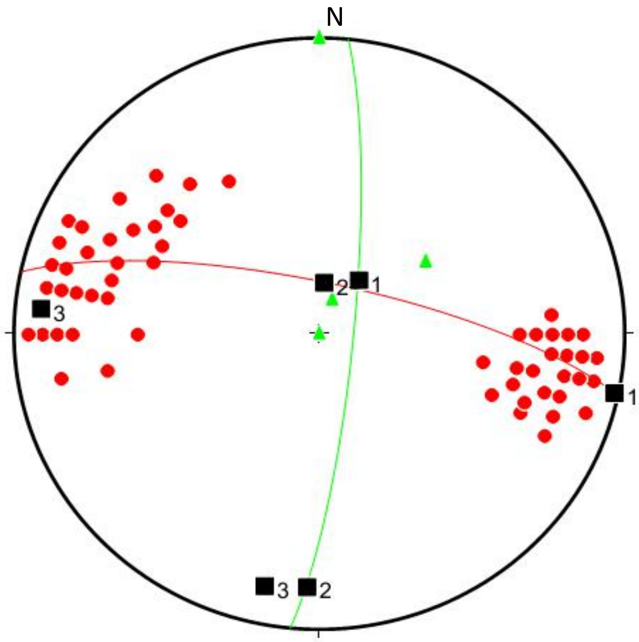

4.8 Equal area plots D1 deformation that shows the relationship between S1 foliation with F1 fold axis of minor folds.

Data symbol:

Red - S1 foliation

Green- F1 fold axis

On the other hand the linear plots shows certain pattern; that is the majority of the poles are generally clustered in southern part of the net. The plunge of linear structures for both fold axis and lineation are clustered dominantly in southrn part of the net.

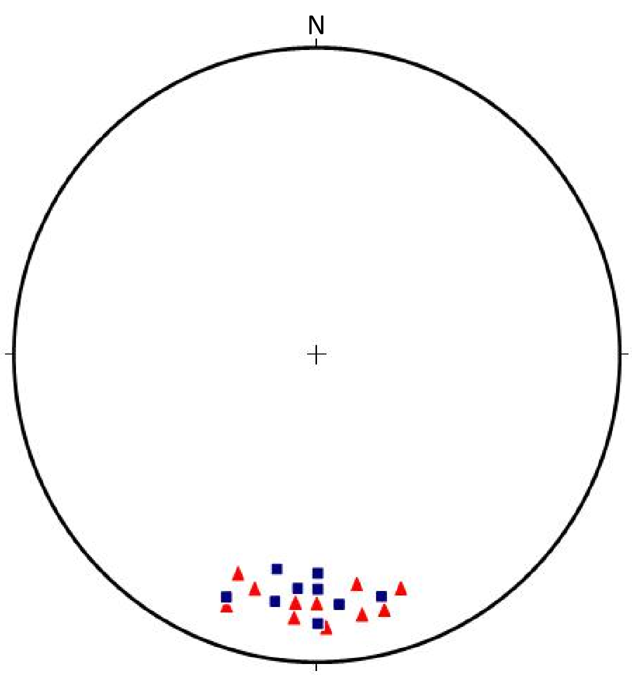

4.9 Equal area plots of D2 deformation that shows the relationship between F2 fold axis and lineation. Number of data 22.

Data symbol:

Red -F2 fold axis

Blue-L2 lineation

Note that both the fold axis and lineation plots shows both plunges towards south at shallow angle (Figure 4.9). The poles to S1 from the main outcrops show a girdle distribution (Figure 4.7), which may imply folding around a gently south plunging axis.

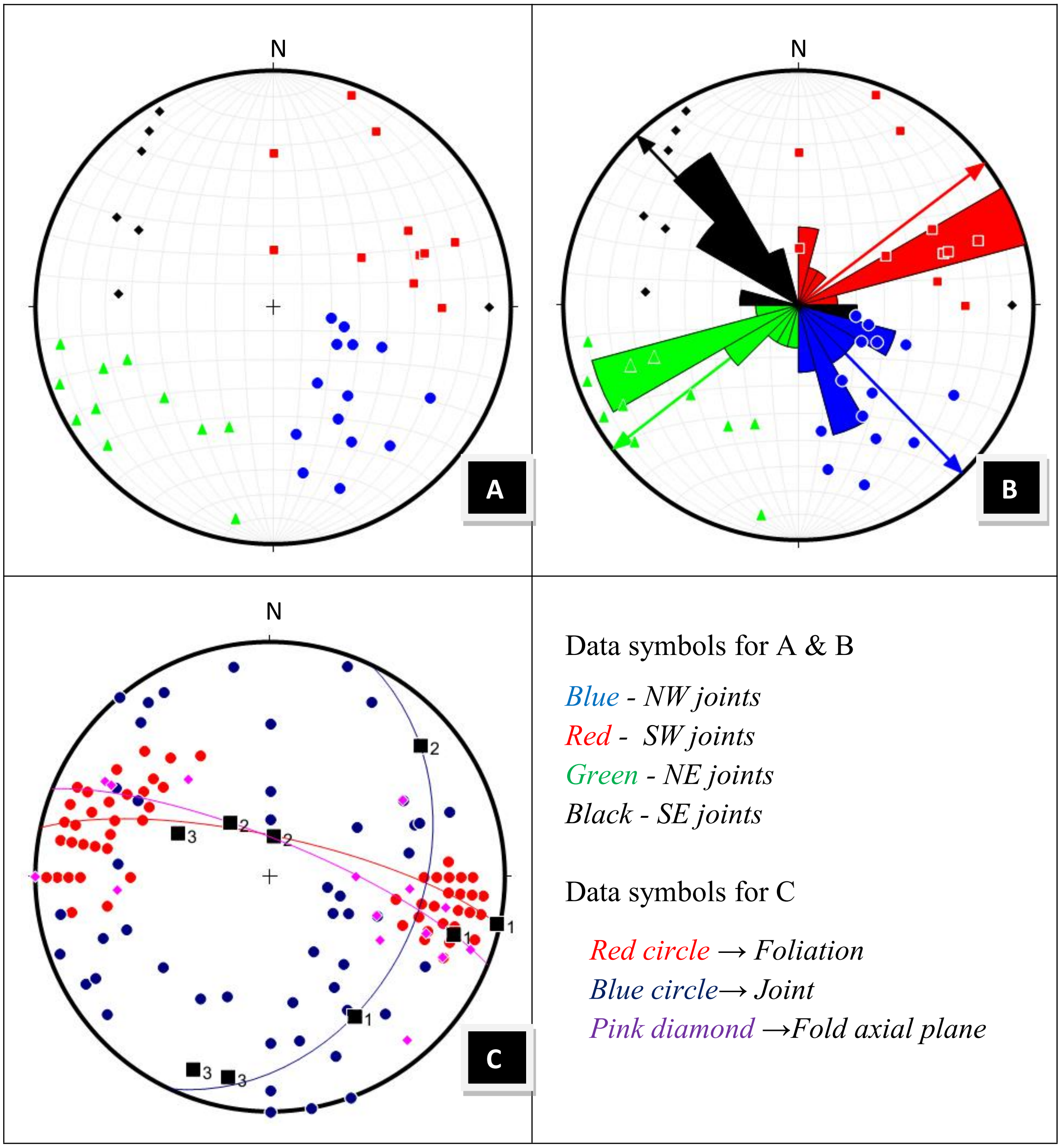

Figure 4.10 A) Equal area plots displays the plots of joints from 50 data as the poles represented by different color that are associated with different set of joint B**)** rose diagram of different sets joint. C) plate C shows the relationship and distribution of poles of various planar structures, such as S1, axial planes of minor folds and joint. The poles are represented by different symbols and color

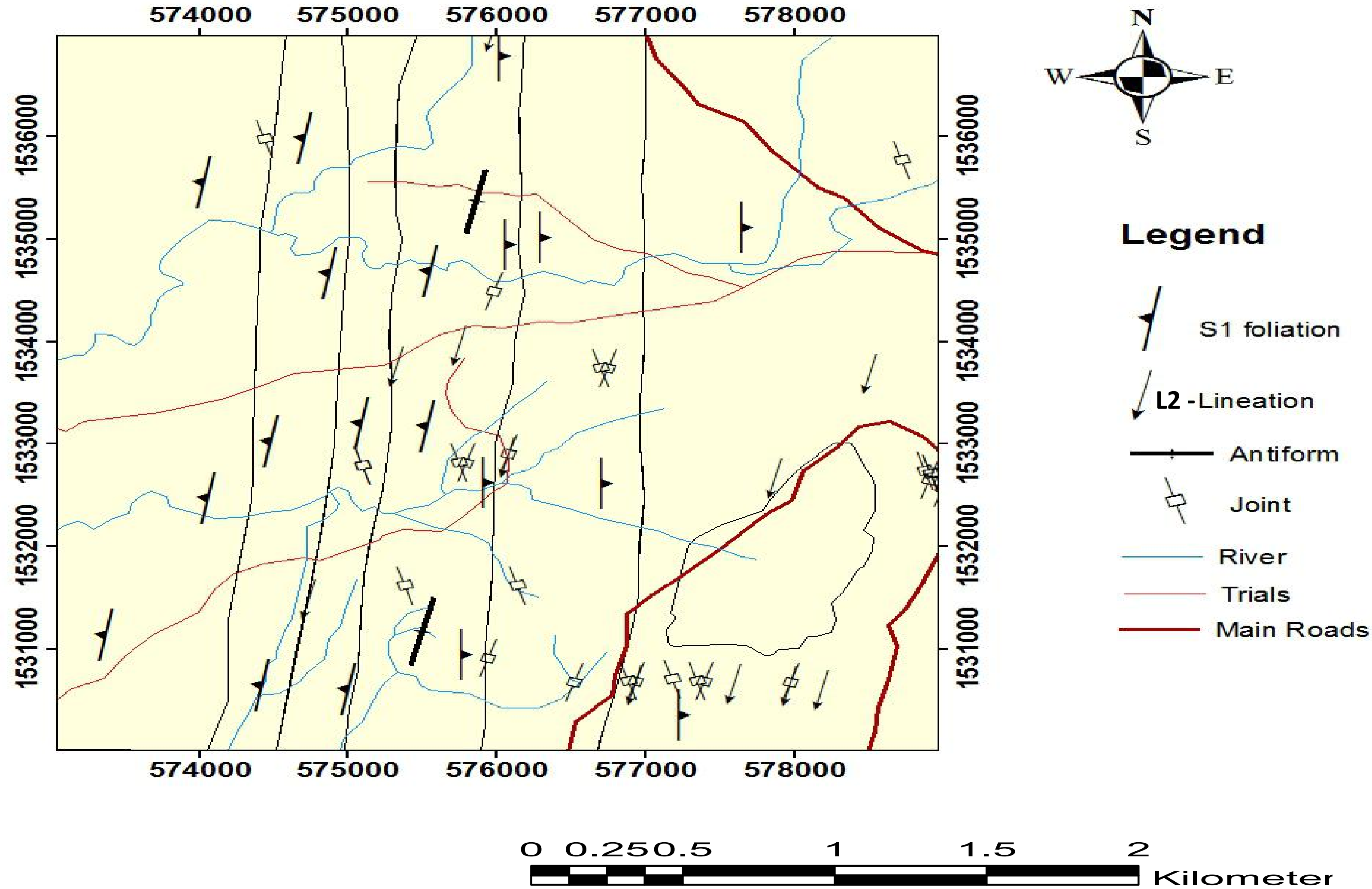

Figure 4.11 Structural map of the study area

CHAPTER FIVE

5. METAMORPHISM AND GEOCHEMISTRY

5.1 Metamorphism

All the studied rocks have been experienced a change in mineralogy and texture indicated by the typical mineral assemblage. These change results new secondary minerals, new texture and rocks. The critical or index mineral assemblage, modal abundance of constituting minerals, the presence of relict mineral and the mineral change by major metamorphic alterations are useful to determine the grade of metamorphism. The thin section examination of the rocks using the above parameter indicate that the study area undergo regionally low grade green schist facies.

The index minerals in the metavolcanic and metavolcaniclastics rocks include epidote, actinolite/tremolite, chlorite, muscovite, sericite and albite. The modal dominance of these minerals is a characteristic feature of low grade metamorphism. Epidote is modally abundant in most of the metavolcanic rocks and occurs as fine to medium grained mineral in the matrix. Chlorite and muscovite are also common in many of the rocks and are probably recrystallized from clay mineral as well as from mafic minerals indicating low grade metamorphism.

Other lower greenschist facies mineral such as actinolite/tremolite also occur as patches associated with chlorite, epidote and calcite mainly in the metabasaltic andesite. The presence of these green color minerals and some relict igneous minerals (like plagioclase and pyroxene) indicate the rock has undergone low grade metamorphism (greenschist facies). The most widely found alterations are epidotization, chloritization, sericitization, actinotilization and carbonitization. These metamorphic alteration produce epidote, chlorite, sericite, actinolite/tremolite and calcite respectively (see table 5.1). In metavolcanic rocks primary minerals like altered K-feldspar and plagioclase are found by preserving their original texture. These mineral are also found altered to secondary mineral like sericite. The presence of recrystallized quartz, sericite, calcite, relict olivine and pyroxene in metavolcanic rocks indicate the low grade metamorphism of the area.

The thin section examination from meta-andesitic units shows the presence of secondary minerals from metamorphic reaction of the minerals originally found in the protolith. These minerals shows replacement feature and are secondary minerals indicating low grade metamorphism of the area. For example chlorite and calcite and calcite and quartz shows replacement (Figure 5.1 A, B & C). In addition, since progressive metamorphism starts from low grade chlorite zone, mafic minerals and muscovite found along with chlorite and epidote in metabasaltic andesite units (Figure 5.1 D). Sericite and calcite are developed from plagioclase and are found as secondary minerals in most of metavolcanic rocks.

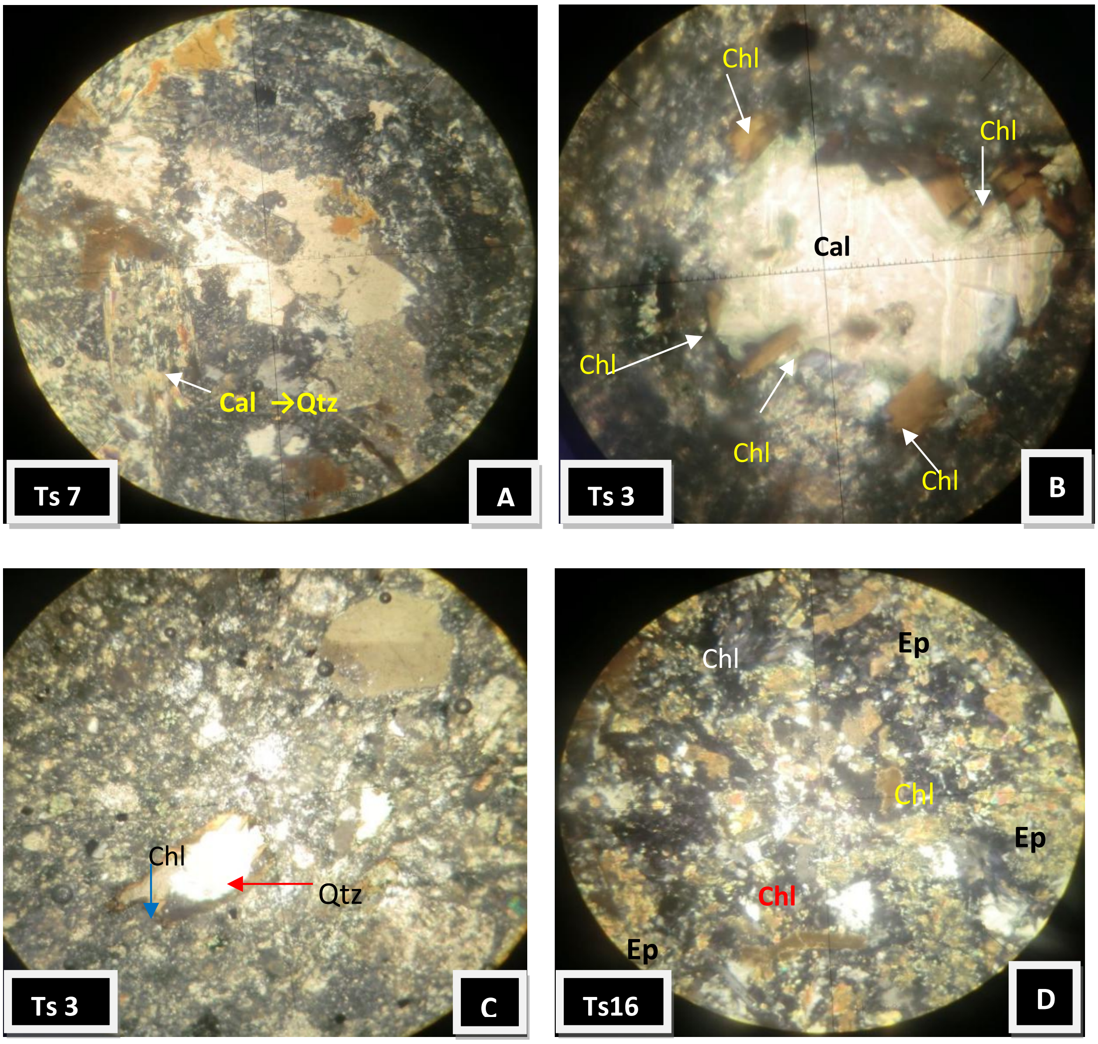

Figure 5.1Mineral replacement features A) partial replacement of calcite by Quartz in metabasaltic andesite units B) replacement of chlorite and calcite in meta-andesitic units C) chlorite, calcite and quartz replacement in meta-andesitic units D) chlorite and epidote minerals indicating chloritization and epidotization in metabasaltic andesite units.(View under XPL,10x10 total magnification, except 40x10 for plate B).

Most of the rock in the study area under thin section shows preservation of some igneous texture with a little alteration. In metavolcaniclastics units especially in slate textural and mineralogical characteristics are more or less similar and shows poorly developed S1 schistosity and weak slaty cleavage. Preservation of compositional layering/primary bedding in slate (see Figure 4.1) is characteristic to low grade metamorphism.

The most dominant critical mineral assemblages of the various rock units are shown below. The underlined ones are considered critical/index the minerals useful to evaluate the grade/facies of metamorphism.

1. Meta-andesitic

   a) Ms + Ep + Ser + Qtz + Pl
   b) Ms + Ep + Chl + Ser + Qtz + Pl
   c) Ser + Ms + Ep + Qtz

2. Metabasaltic andesite

   a) Ep + Act/Tr + Chl+ Qtz + Pl
   b) Chl + Ser + Ms + Kfs + Pl

3. Metabreccia

   a) Ser + Chl + Ms + Ep + Qtz

4. Tuffaceous layer

   a) Ser + Ms + Qtz + Kfs

5. Slate

   a) Ser + Chl + Ms + Ep + Qtz
   b) Chl + Ser + Kfs + Qtz

These assemblages demonstrate that the rocks underwent regional metamorphism in the lower green schist facies. Regionally these rocks of Tsaliet metavolcanics in northern Ethiopia were correlated with the peak regional metamorphism at pumpellyite–actinolite to lower greens schist facies (Alene, 1998; Alene and Sacchi, 2000).

5.1.1 Time relation between deformation and metamorphism

As mentioned in chapter four microscopic examination of thin section from different units revealed different fabric that developed due to different phases of deformation. Two planer structures are indentified from field and petrographic studies (S0 and S1). S2 schistosity is poorly developed but can be observed by re-alignment of some minerals. The formation and orientation relationship of some selected mineral can explain the metamorphic event and the time relation between deformation and metamorphism.

Mineral like Quartz, muscovite, sericite and chlorite shows alignment with earlier S1 schistosity that is formed during D1. So it can be said that the M_1 metamorphic event is responsible for the formation of these minerals which is synchronous with the D1 deformation phases (Figure 5.2). The presence of chlorite and epidote along with mafic mineral can define the prograde metamorphic event since prograde metamorphism starts from low grade chlorite zone (see Figure 5.1 D). These minerals associated with the M1 metamorphic event mostly found as fine to medium grained recrystallized and altered form.

The above listed mineral however underwent slight rotation and recrystallization after D1 or synchronous to D2 and marks M_2 metamorphic event. Sericite, chlorite, calcite and quartz show relatively strain free and they are secondary mineral formed during M2 (Figure 5.2).

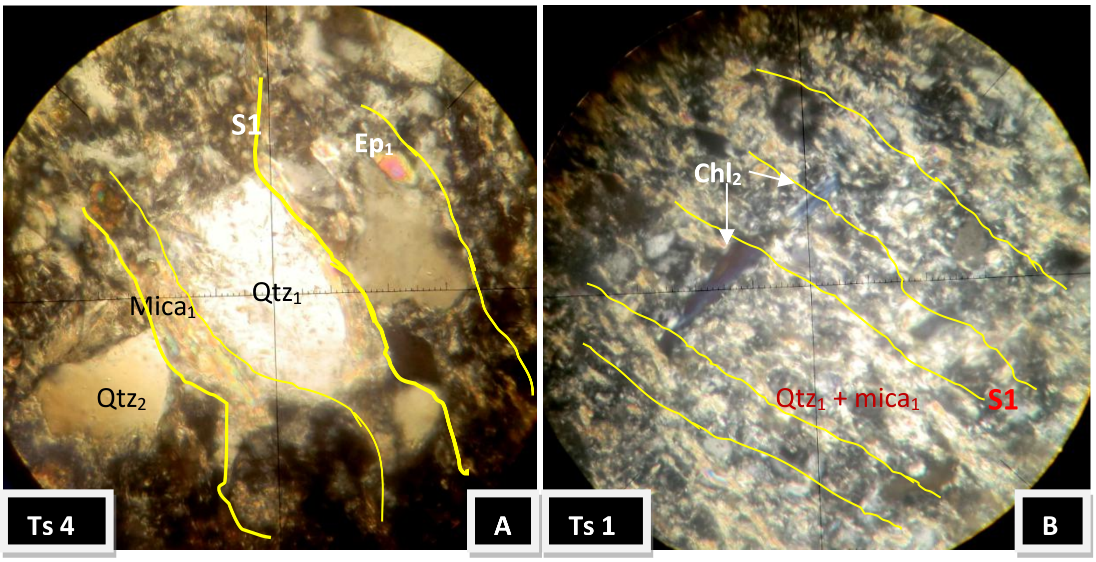

Figure 5.2 Microphotograph showing Mineral alignment and rotation A) the development of S1 schistosity deflecting around recrystallized quartz grain and re-

alignment of secondary quartz grain in meta-andesitic units. Notice the fine grained mica shows slight deflection around quartz grain; B) secondary chlorite crystal show rotation along S1fabric in slate. (View under XPL, 10x10 total magnification for both).

Table 5.1 M1 and M2 metamorphism with associated deformation phases and mineral assemblage.

M1 coeval to D1	M2 coeval to D2
Mineral assemblage	Mineral assemblage
$Chlorite_1$	$Chlorite_2$
$Epidote_1$	$Epidote_2$
$Quartz_1$	$Quartz_2$
$Muscovite_1$	$Sericite_2$
$Calcite_1$	$Calcite_2$

5.2 Geochemistry

5.2.1 Analytical Methods

Philips X-ray fluorescence spectroscopy model PW 2400 was used to analyze major, minor and trace elements in the pellets. The rock samples are crushed using aluminum jaw crusher and pulverized by agate disc grinder to -200 mesh consequently fused and pressed pellets are prepare and excited with x-ray radiation, that normally generated by an x-ray tube operated at a potential between 10 and 100 kilo volt.

The reason why fused pellets are prepared mainly for major elements and pressed pellets for minor and trace elements is that in preparation of the pressed pellets the amounts of foreign substances has to be low so that the concentration of trace elements will not get further diluted; and the analysis does not show below detection limit, but during the preparation of fused pellets there are different admixture to the sample. Since it is a major element analysis expressed in percent, it will not affect concentration of the element so much.

Detection limits for many of these trace elements lie in the range of 1-10 ppm, under routine operating conditions. Every sample is analyzed utilizing the whole rock analysis.

5.2.2 Major and Trace Element Characteristics

The metavolcanic rocks of the study area have sub-alkaline to alkaline chemistry. The SiO2 contents ranges between (51.43-58.06 wt.%). All samples can be classified as low-silica andesite (51–58 wt.% SiO2), and the samples also fall in the metabasaltic andesite and meta-andesite fields of the conventional alkali–silica diagrams (Figure 5.6).

Most samples show high-alumina (Al2O3) contents from 12.39 up to 14.39 wt %, similar to those of calc-alkaline series rocks. Iron content (Fe2O3) seems to be relatively high ranging between 8.29 and 10.39 wt %. The high iron contents appear to reflect an abundant secondary opaque phase (magnetite?). TiO2 values are generally < 1 %, therefore they are in the range accepted in calc-alkaline lavas (Pearce and Cann, 1973).

The abundances of Na2O (mostly 1.80 –4.10 wt %), K2O (0.78 – 2.45 wt %), P2O5 (0.23–0.32 wt. %) and the Na2O/K2O (mostly between 1 and 3) are low. This can be attributed to a loss during alteration and metamorphism (Alene and Sachi, 2000a). The majority of samples show relative high abundance of MgO ranging between 4.57 to 8.43 and CaO ranging between 1.83 to 9 wt % which may be related to the presence of Mg rich chlorite, epidote and the non-intensive metamorphism (Alene and Sachi, 2000a).

In terms of trace elements content (Table 1), with the exception of Sr (205-716 ppm), Y (23-25 ppm), their abundance is generally low Nb (3 -8 ppm), Ba (348- 455 ppm) and Zr (100-182 ppm), feature suggesting the generation of these rocks within active plate margin (Pearce and Gale, 1977). Although there is lack of some trace element result as shown in table 1, the ratios of (Niobium with Yttrium) Y/Nb and Nb/Y fall in the range between 3.12 -8 and (0.12-0.32) respectively and Nb/Y is < 1.0 implying possible approach to calc-alkaline and tholeiitic affinities (Lissan et al., 2010).

Table 5.2: Representative major, minor and trace element geochemical data for metavolcanic rocks of the Atsbi area.

Sample	Units	Ch1 T8	Ch3 T4	Ch4 T6	Ch5 T8	Ch6 T8
SiO2	%	58.06	53.29	52.42	51.43	56.35
Al2O3	%	14.02	13.61	12.81	12.39	14.39
Fe2O3	%	10.39	9.03	11.44	8.29	8.77
CaO	%	1.83	5.70	4.44	9.01	3.31
MgO	%	4.57	5.23	8.43	5.50	4.88
Na2O	%	4.10	2.55	3.45	1.80	2.68
K2O	%	1.48	2.08	0.78	1.42	2.45
TiO2	%	0.69	0.63	0.93	0.57	0.66
MnO	%	0.15	0.19	0.18	0.14	0.13
P2O5	%	0.24	0.24	0.32	0.25	0.23
LOL	%	4.22	7.22	4.45	8.94	5.93
Total	%	99.75	99.77	99.65	99.74	99.78
Sr	Ppm	222	327	716	266	205
Sc	Ppm	12	12	12	12	12
Y	Ppm	25	25	23	24	25
Ba	Ppm	426	404	348	404	455
Zr	Ppm	133	106	182	100	109
Nb	Ppm	8	4	5	3	4
Mo	Ppm	<5	<5	<5	<5	<5
Pb	Ppm	33	33	31	35	33
Zn	Ppm	90	79	79	63	78
Co	Ppm	29	26	33	17	21
Cu	Ppm	88	19	50	33	20

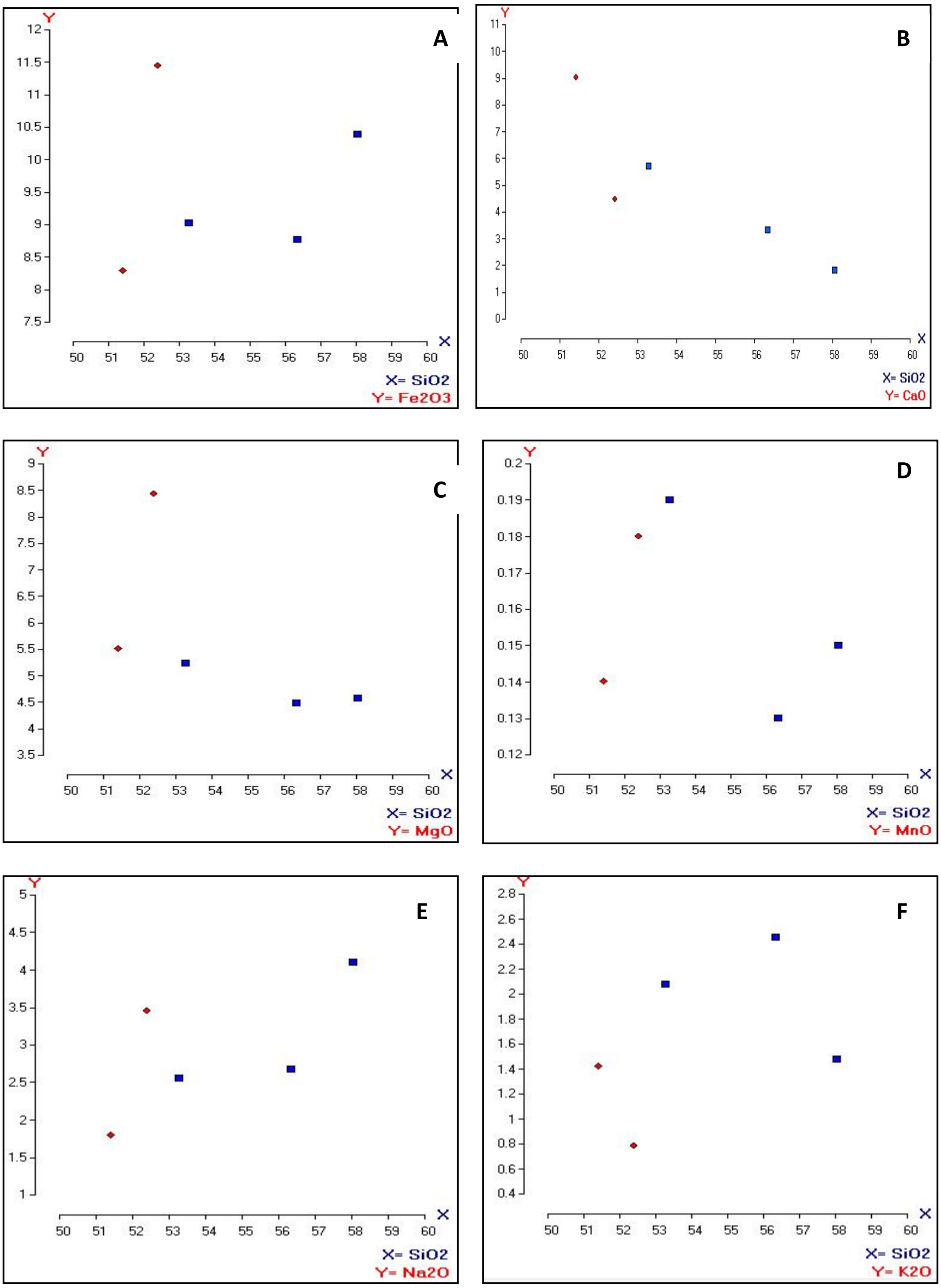

Figure 5.3. Harker-type variation diagrams showing SiO_2 variation diagrams for various major/minor element oxides (in wt%), A) Al_2O_3, B) Fe_2O_3, C) Na_2O, D) K_2O, E) MgO, and F) Mno (Symbols: Closed rectangle = meta-andesite and closed cubic box = meta basaltic andesite.

Selected major elements and trace elements are plotted against SiO_2 on Harker variation diagrams (Figure 5.3 & 5.4). Compatible major oxides Fe_2O_3, CaO, MgO and MnO (Figure 5.3 A, B, C & D) show negative correlation which indicate normal differentiation tending to decrease as SiO2 increases. This suggests calcic plagioclase, olivine, pyroxene and magnetite were major fractionating phases during evolution of the magma. Other major oxides (not shown here) are poorly correlated with SiO2. A broad positive correlation of Na2O and K2O with increasing SiO2 concentration is observed which are incompatible with the presence of mafic minerals.

The majority of the trace elements analyzed show moderate positive correlations with silica. Plots of SiO2 versus some selected compatible and incompatible trace elements concentrations are illustrated in Figure 5.4. A moderate negative correlation is observed between Co, Cu and Sr (Figure 5.4 B & D) and other compatible trace elements with SiO2, suggesting partitioning of olivine, spinel and pyroxene. Ba, Nb, Zn, Zr and Y show positive correlation on variation diagrams of elements plotted against silica (Figure 5.4 A, C, E and F).

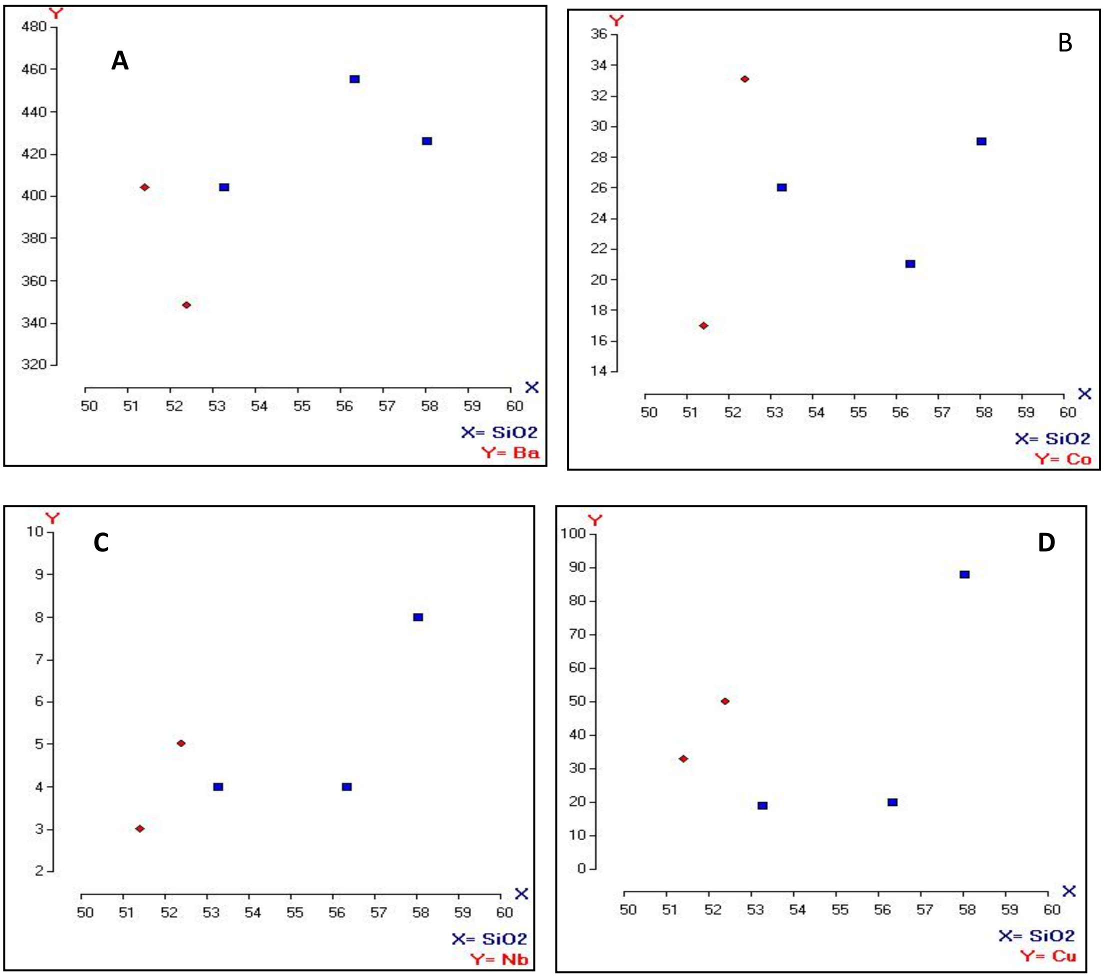

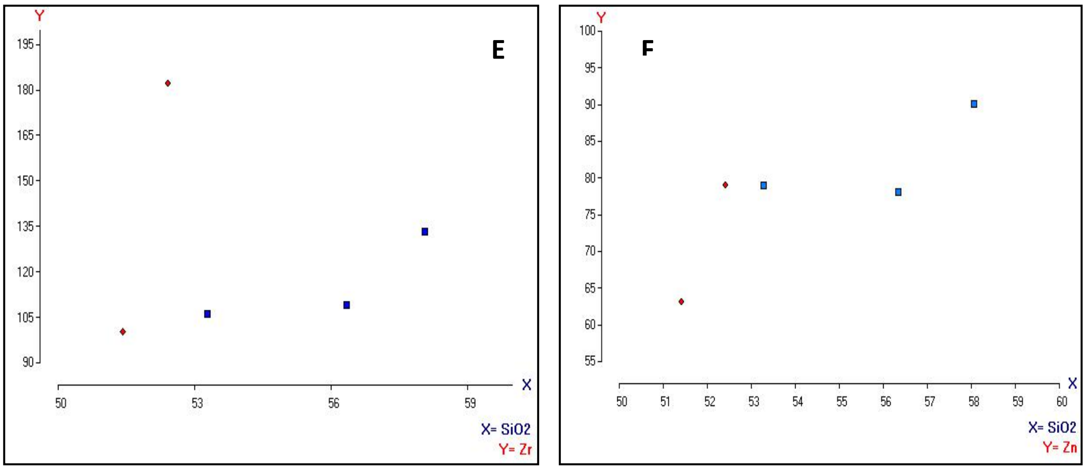

Figure 5.4 Harker-type variation diagrams showing the variation in A) Ba, B) C0, C) Nb, D) Cu, E) Zr, and F) Zn with respect to SiO2 for the rocks of study area. (Symbols: as in figure 5.3).

In the multi-element diagram (Figure 5.5A) normalized to primitive mantle values of McDonough and Sun (1995), the trace element data show that the rocks possess a calc-alkaline island arc trace element patterns, enriched incompatible large ion lithophile elements (LILE: Sr, and Ba) relative to high field strength elements (HFSE: Zr, Y, Ti, and Nb) contents, that show a negative Nb anomalies. In the chondrite-normalized REE pattern (Figure5.5B), values of (Wood et al., 1979), all the analyzed rocks samples display enrichment in Ba, Zr, Sc, Nb and Y) contents relative to heavy rare earth elements Mn, P, K, Co and Ti) contents. The Pattern generally shows steep, moderately irregularities.

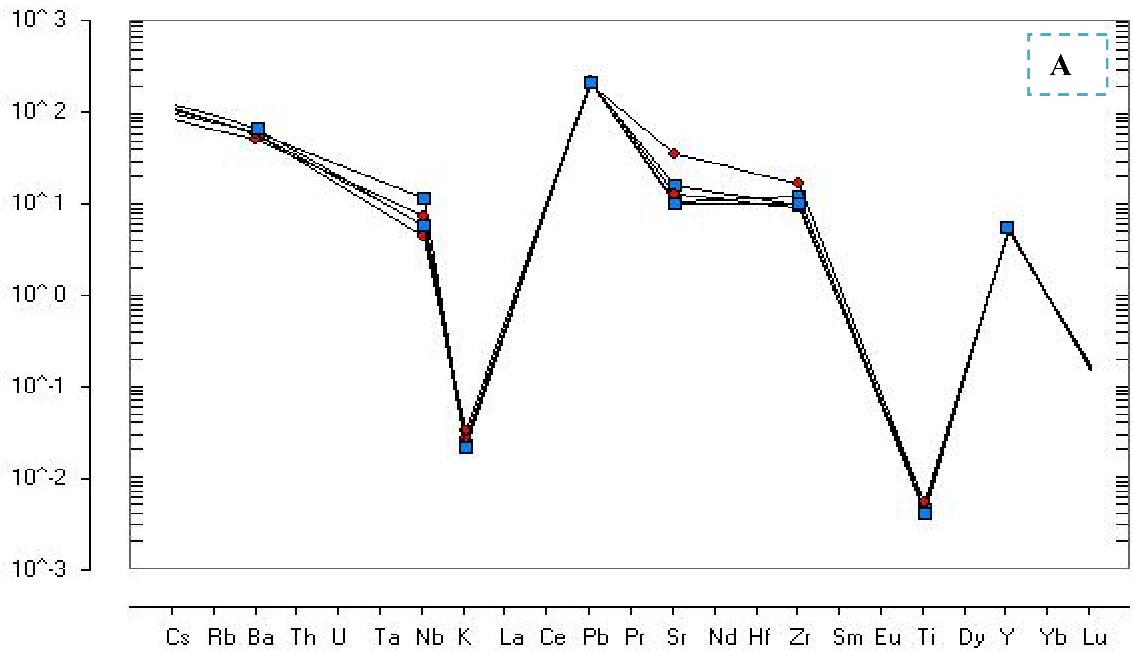

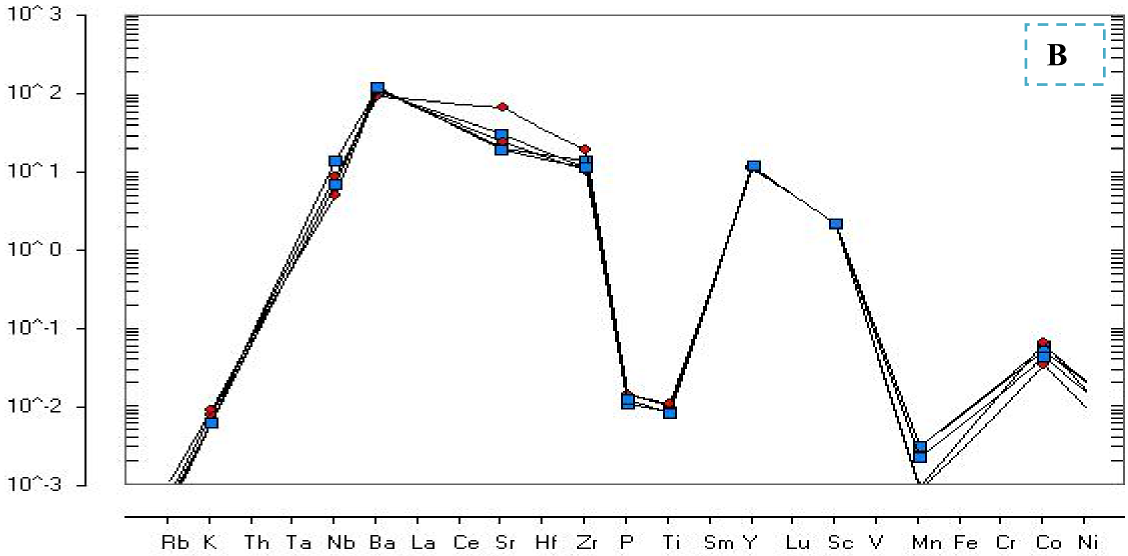

Figure 5.5 (A) Primitive mantle-normalized multi-element plots. The order of the elements and normalizing values are from Sun and McDonough (1995), (B) Chondrite diagram of the rock samples from the study area (After Wood et al., 1979) (Symbols: as in Figure 5.3).

5.2.3 Tectonic setting of the metavolcanic rocks of Atsbi area

All the metavolcanics plotted on the total alkali versus silica diagram of Le Bas et al., 1986 (Figure 5.6) clear that the metavolcanic rocks are principally identified as low-silica andesite (51– 58 wt. % SiO2) and two samples fall in the basaltic andesite field.

There are several geochemical approaches to distinguish whether rock sample belong to an island-arc tholeiite (IAT), calc-alkaline basalt (CAB) or mid-ocean ridge basalt (MORB). The mafic/intermediate rocks also show predominantly calc-alkaline affinity (Figure 5.8). The occurrence of calc-alkaline rocks in an island arc setting has long been attributed to a mature stage of arc evolution (e.g. Jakes and White, 1971; Miyashiro, 1974 sited by Alene et al., 2000).

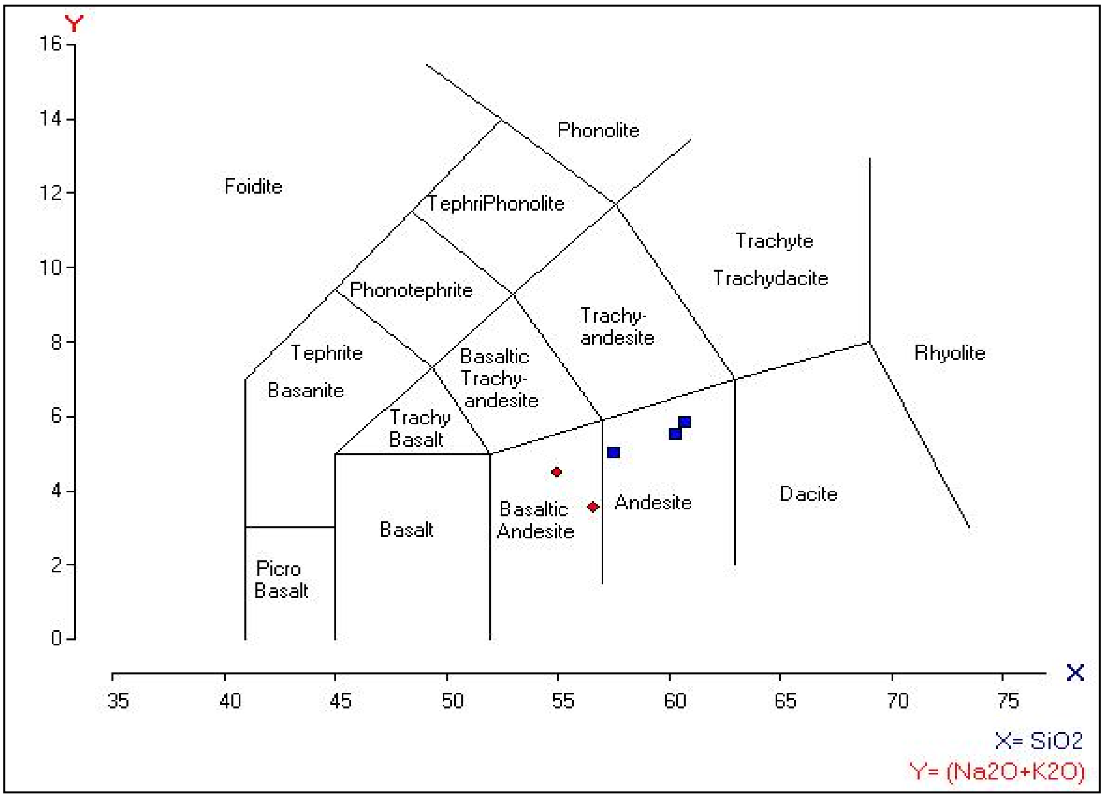

Figure 5.6 Chemical classification diagram based on TAS (wt %) (Na2O + K2O vs. SiO2) of LeBas et al., (1986) (Symbols: as in Figure 5.3)

The relationship between SiO2 and K2O contents (Middlemost, 1975) of all the metavolcanic rocks indicates the transition between the alkalic and sub-alkalic fields (Figure 5.7). A low Nb content (< 9 ppm see table 5.1) is considered typical of subduction-related basaltic rocks (Woldehaimanot, 2000).

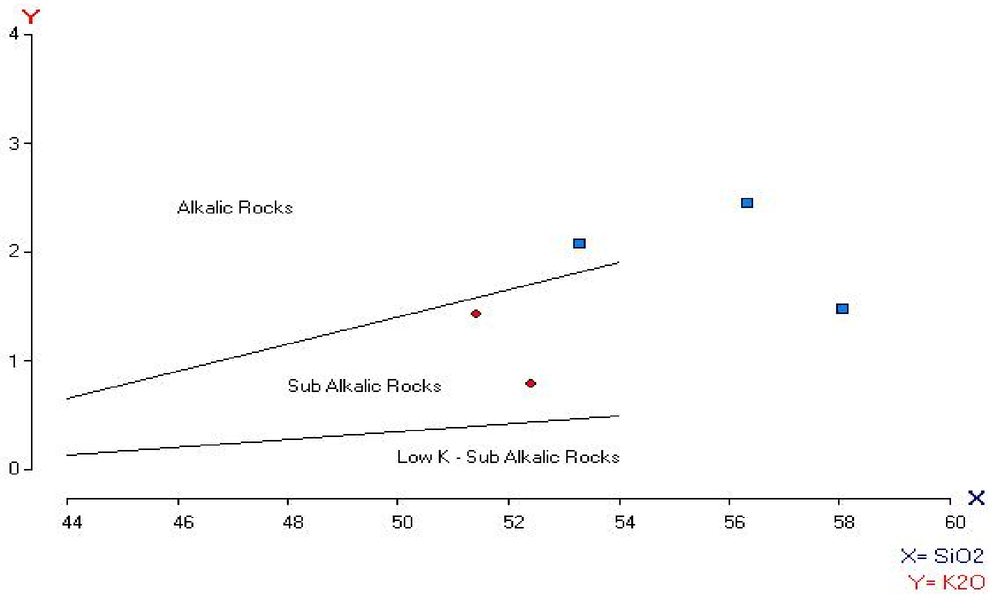

Figure 5.7 K2O vs. SiO2 plot (Middlemost, 1975) illustrating sub-alkaline to alkaline trends (Symbols: as in Figure 5.3).

The Zr-Nb-Y diagram (Meschede, 1986) (Figure 5.9B) shows that all the metavolcanic rocks lie on 'C', which is within plume tholeiites volcanic arc basalt field.

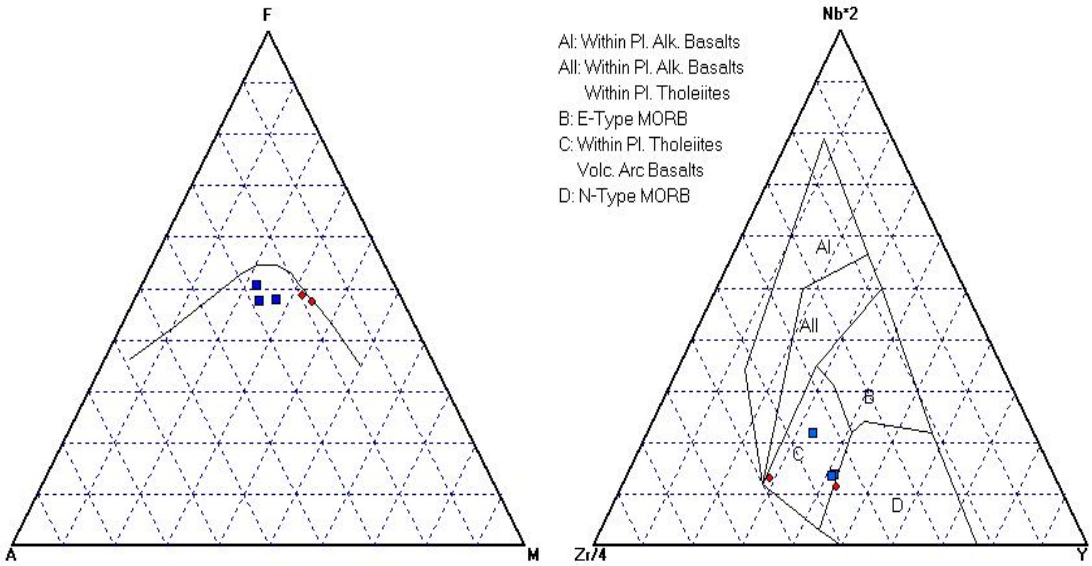

Figure 5.8 A) an AFM triangular discrimination diagram for the rock samples (after Irvine and Baragar, 1971); B) Zr-Nb-Y discriminant diagram (after Meschede, 1986) used for the Atsbi area metavolcanics. (Symbols: as in Figure 5.3).

The geology of the Atsbi area is characterized by predominantly low-grade metavolcanic rocks where dominantly metamorphic rocks are from volcanic protoliths as disclosed from the field, petrographic work and geochemical signature. There is no sufficient geochemical data for precise and detail determination of tectonic setting of the Atsbi area, as the number of analyzed geochemical samples is small. However, the limited present geochemical results and analysis are almost consistent with the previous investigations. The major element oxide and trace element data for the metavolcanic rocks of Atsbi area show a small range of composition indicating that they may have originated from a single, chemically uniform parent melt. Generally, many authors (e.g. Alene et al., 1998; Asrat et al, 2001; Avigad et al., 2007; Kazmin, 1973; ; Miller et al., 2012; Tadesse et al., 1999; Tadesse et al.2000; Teklay, 1997; Woldehaimanot, 2000) shows the Tsaliet Group of northern Ethiopia represents an arc volcanics sequence or subduction-related arc accretion of the ANS.

CHAPTER SIX

6. CONCLUSION AND RECOMMENDATION

6.1 Conclusion

The study area comprises poly deformed and metamorphosed low grade metamorphic rocks that are also affected by later brittle deformation and quartz vein. The map area is represented by extensively exposed metavolcaniclastics unit consists of metabreccia, tuffaceous layer and slate of pyroclasic origin and metavolcanic consists of metabasaltic andesite to meta-andesitic units. Three generations of quartz veins occur in the study area cutting and/or parallel to S1 foliation. The first generation quartz veins are folded by D2 and less abundant as compared to the unfolded second and thrid generations. The second generation are that runs parallel to the regional foliation. The third generation of quartz veins are found associated with joints and fractures and crosscut the regional trend.

In this paper, the results of petrographic, structural and kinematic analyses show that the metavolcanic rocks of Atsbi area is affected by two phases of ductile deformation (D1 and D2). D1 deformation resulted in NE oriented foliations as well as sub vertical to vertical folds. D2 deformation caused the local development of open, upright and harmonic low plunging folds. NW, SW and also NE trending mederate to sub vertical dipping joint post-date ductile deformation. Therefore, it can be conclude that the brittle deformation is younger than the foliations and the region experienced a ductile to brittle transition deformation. These features are very similar to the structural features described in collision/accretion related setting in the Arabian Nubian shield (Berhe, 1990; Abdelsalam and Stern, 1996; Stern, 1994).

The metavolcanic rocks are locally affected by propylitic alteration and sericitization. The main alterations experienced by these rocks are pervasive sericitization, epidotization, silicification, and chloritization. The index mineral assemblage from MV and to some extent MVC rocks such as epidote, tremolite/actinolite, chlorite, muscovite, sericite and calcite demonstrate lower green schist facies of metamorphism of the study area. Two metamorphic event are identified associated with the D1 and D2 ductile deformation. M1 metamorphic event is related to those minerals that shows alignment with the S1 foliation synchronous with D1 deformation.

The rotation of minerals , recrystallization and prograde metamorphism which are post tectonic to D1 and pre tectonic to D2 mark the M2 metamorphic event in the area.

The local geochemical data of the metavolcanic rocks of Atsbi area is provided in an attempt to determine the tectonic domain of the area within the Tsaliet Group of Arabian-Nubian Shield. The major, minor and trace element patterns of the metavolcanic rocks of the study area support the hypothesis that they are derived from the arc volcanics sequence or subduction-related arc accretion. All the samples plotted on the chemical classification diagram clear that the samples of the metavolcanic rocks are principally identified as low-silica andesite and only a few samples fall in the basaltic andesite field. The calk alkaline nature of the rocks of Atsbi area on the Zr-Nb-Y diagram shows that all the metavolcanic rocks lie within plume tholeiites volcanic arc basalt field. Generally the small compositional range of the samples indicate that the metavolcanic rocks of Atsbi area originate from uniform parent melt. These results contribute to the better understanding of the least studied and undifferentiated part of the Tsaliet Group in relation to the lithologic association, metamorphism and deformation.

6.2 Recommendations

- Since Atsbi area is the least studied and undifferentiated part of the Tsaliet Group, the first recommendation goes on in strengthens the geochemical data with more sample in order to have better understanding of the area in terms of tectonic setting.
- The feature study in this area should be accomplished in large scale mapping for stratigraphic correlation with the Tsaliet Group of adjacent area and also to the southern province of the Arabian Nubian Shield.

REFERENCES

Abdelsalam, M.G. and Stern, R.J. (1996). Sutures and shear zones in the Arabian-Nubian Shield, Journal of African Earth Sciences. **23**: 289-300.

Alene, M., (1998). Tectono-magmatic evolution of the Neoproterozoic rocks of the Mai Kenetal–Negash area, Tigrai, northern Ethiopia. Unpublished Ph.D. Thesis, University of Turin.

Alene, M., Ruffini, R., Sacchi, R., (2000). Geochemistry and geotectonic setting of Neoproterozoic rocks from northern Ethiopia (Arabian–Nubian Shield). Gondwana Res. 3, 333–347.

Alene, M., Jenkin, G.R.T., Leng, M.J., Darbyshire, D.P.F., (2006). The Tambien Group of Ethiopia: an early Cryogenian (ca. 800–735 Ma) Neoproterozoic sequence in the Arabian–Nubian shield. Precambrian Research 149, 79–89.

Arkin, Y., Beyth, M., Dow, D.B., Levitte, B., Temesgen, H.,Tsegaye H., (1971). The Geological map of Mekele area (1:250,000). Ministry of Mines, Addis Ababa.

Asrat.A, p.Barbery, and G.Gleizes., (2001). Precambrian geology of Ethiopia: a review. African Geoscience.

Asrat A., Gleizesc G., Barbeya P., and Ayalew D. (2003). Magma emplacement and mafic–felsic magma hybridization: structural evidence from the Pan-African Negash pluton, Northern Ethiopia, Journal of Structural Geology. **25**: 1451-1469.

Asrat, A., Barbey, P., Ludden, J.N., Reisberg, L., Gleizes, G., Ayalew, D., (2004). Petrology and isotope geochemistry of the Pan-African Negash Pluton, northern Ethiopia; mafic-felsic magma interactions during the construction of shallow-level calcalkaline plutons. Journal of Petrology 45, 1147–1179.

Avigad, D., Stern, R.J., Beyth, M., Miller, N., McWilliams, M., (2007). Detrital zircon U–Pb geochronology of Cryogenian diamictites and lower Palaeozoic sandstone in Ethiopia (Tigrai): age constraints on Neoproterozoic glaciation and crustal evolution of the southern Arabian–Nubian Shield. Precambrian Research 154, 88–106.

Ayalew, T., Bell, K., Moore, J.M., and Parrish, R.R., (1990). U-Pb and Rb-Sr geochronology of the Western Ethiopian Shield. Geological Society America Bulletin 102, 1309-1316.

Blanford W.T. (1870). Observations of the geology and zoology of Abyssinia made during te progress of the British expendition to that country in 1867-1868. Macmillan. London.

Berhe S.M. (1990). Ophiolites in northeast and east Africa: Implications for Proterozoic crustal growth, Journal Geological Society London. **147**: 41-57.

Beyth, M. (1971) The geology of central and western Tigre. Unpub.report, Ministry of Mines, Addis Ababa.

Beyth, M., (1972). The Geology of Central Western Tigre, Ethiopia. University of Bonn, p. 155.

Beyth, M., Avigad, D.,Wetzel, H.U., Matthews, A., Berhe, S.M., (2003). Crustal exhumation and indications for Snowball Earth in the East African Orogen: North Ethiopia and East Eritrea. Precambrian Research 123, 187–201.Faure, G., 1986. Principles of Isotope Geology. Wiley, New York.

De Wit, M.J. and Chewaka, S. (1981). Plate tectonic evolution of Ethiopia and origin of its mineral deposits: an overview In: Chewaka, S. and de Wit, M.J. (eds) Plate tectonics and metallogenesis: some guidelines to Ethiopian mineral deposits, Ethiopian Institute of Geological Surveys. Bulletin 2: 115–129.

Garland, C.R., (1980). Geology of the Adigrat Area. Geological Survey of Ethiopia, Memoir1, 51 p.

Gebresilassie, S.G,. (2009). Nature and characteristics of metasedimentary rock hosted gold and base metal mineralization in the Workamba area, central Tigray, northern Ethiopia. Phd thesis.

Irvine, T. N. and Barager, W. R. A. (1971). A guide to the chemical classification of the common volcanic rocks. Canadian Journal of Earth Science. 8: 523-548.

Jakes, P. and White, A.J.R. (1971). Composition of island arcs and continental growth. Earth Planet. Sci. Lett., v. 12, pp. 224-230.

Johnson, P.R., Woldehaimanot, B., (2003). Development of the Arabian–Nubian Shield: perspectives on accretion and deformation in the northern East African Orogen and the assembly of Gondwana.

Johnson, P.R., Abdelsalam, M.G., Stern, R.J., (2003). The Bi'r Umq-Nakasib suture zone in the Arabian–Nubian Shield: a key to understanding crustal growth in the East African Orogen. Gondwana Research 6, 523–530.

Kazmin, V. (1971). Precambrian of Ethiopia. Nature 230, 176-177.

Kazmin, V. (1972). Geological Map of Ethiopia. 1:2,000,000, Ministry of Mines and Energy, Addis Ababa, Ethiopia.

Kazmin, V. (1973). The geological map of Ethiopia, 1:2,000,000. Ethiopian Institute of Geological Surveys, Addis Ababa, Ethiopia.

Kazmin, V., Shiferaw, A., Balcha, T., (1978). The Ethiopian basement: stratigraphy and possible manner of evolution. Geologische Rundschau 67, 531–548.

Kennedy, W.Q. (1964). The Structural differentiation of Africa in the Pan-African (±500 m.y). Tectonic episode: Res. Inst. Afri. Geol., University of Leeds, 8th ann. Rep., p. 48-49.

Kroner A., (1980). Pan African crustal evolution. Updated and modified version of a paper presented, Cairo, Egypt, October. Episode, Vol. 1980, No.2

Kroner, A.,Linnebacher, P., Stern, R.J., Reischmann, T., Manton, W., and Hussein, I.M., (1991). Evolution of Pan-African island arc assemblages in the southern Red Sea Hills, Sudan, and in south-western Arabia as exemplified by geochemistry and geochronology. Precambrian Research 53, 99-118.

Kroner, A., and Stern, R.J., (2005). AFRICA/Pan- African Orogeny. Encyclopedia of Geology,v.1.Elsevier,Amsterdam,www.utdallas.edu/~rjstern/pdfs/PanAfrican Orogeny.pdf. viewed 7Nov2012.

Le Bas, M. J., Le Maitre, R. W., Streckeisen, A. and Zanettin, B. (1986). A chemical classification of volcanic rocks based on the total alkali–silica diagram. Journal of Petrology. 27: 745–750.

Levitte D., (1970). The geology of central part of Mekelle sheet (ND37-11). Ethiopian Institute of Geological Survey. Note No. 821-201-12: 66.

Lissan, N.H. and Bakheit, A.K. (2010). The Geology and Geochemistry of Metavolcanic Rocks from Artoli Area, Berber Province, Northern Sudan: An Implication for Petrogenetic and Tectonic Setting. Journal of American Science. 6(8).

McDonough, W. F. and Sun, S. S. (1995). The composition of the earth. Chemical Geology. 120: 223-253.

McWilliams (1981). Palaeomagnetism and Precambrian tectonic evolution of Gondwana. In Precambrian Plate Tectonics, ed. A Kr6ner, pp. 649-87. Amsterdam: Elsevier.

Mengesha Tefera., Tadiwos Chernet and Workineh Haro. (1996). Explanation of the Geological map of Ethiopia. Ethiopian Institute of Geological Survey.

Meschede, M. (1986) A method of discrimination between different types of mid-ocean ridge basalts and continental tholeiites with the Nb-Zr-Y diagram. Chem. Geol., v. 56, pp.

Middlemost, E.A.K. (1975). The basalt clan. Earth Science Reviews. 11: 337-364.

Miller, N.R., Alene, M., Sacchi, R., Stern, R., Conti, A., Kröner, A., Zuppi, G., (2003). Significance of the Tambien Group (Tigre.N. Ethiopia) for Snowball Earth Events in the Arabian–Nubian Shield. Precambrian Research 121, 263–283.

Miller N. R., Robert J. Stern, Dov. Avigad, Michael Beyth, Bettina Schilman (2009). Cryogenian slate-carbonate sequences of the Tambien Group, Northern Ethiopia (I): Pre-“Sturtian” chemostratigraphy and regional correlations. Precambrian research.

Miller, N.R., Avigad, D., Stern, R.J. and Beyth, M. (2011).The Tambien Group, Northern Ethiopia (Tigre), Geological Society of London. **36**: 263-276.

Miyashiro, A. (1974). Volcanic rock series in island arcs and active continental margins. Amer. J. Sci., v. 274, pp. 321-355.

Pearce, J. A. and Cann, J. R., (1973). Tectonic setting of basic volcanic rocks determined using trace element analyses. Earth and Planetary Science Letters. 19: 290–300.

Pearce, J.A. and Gale, G.H., (1977). Identification of ore- deposition environment from trace-element geochemistry of associated igneous host rocks. In: Volcanic Processes in Ore Genesis. Institute Mining Metallurgy, Geological Society London, Special Publication 7, pp. 14-24.

Pearce, J.A., Harris, N.B.W., Tindle, A.G., (1984). Trace element discrimination diagrams for the tectonic interpretation of granitic rocks. Journal Petrology 25(4), 956-983.

Sifeta, K., Roser, B.P., Kimura, J.I., (2005). Geochemistry, provenance, and tectonic setting of Neoproterozoic metavolcanic and metasedimentary units, Werri area, Northern Ethiopia. Journal of African Earth Sciences 41, 212–234.

Shackleton, R.M. (1986). Precambrian collision tectonics in Africa. In: Collision Tectonics, (Edited by Coward, M.P. and Ries, A.C.), Geological society, London, special publication. 19: 329-34.

Stern, R.J., (1994). Arc assembly and continental collision in the Neoproterozoic East African Orogen: implications for the consolidation of Gondwanaland. Annual Reviews of Earth and Planetary Sciences 22, 319–351.

Stern, R.J., (2002). Crustal evolution in the East African Orogen: a neodymium isotopic perspective. Journal of African Earth Sciences 34, 109–117.

Tadesse A., (1998). Geochemistry of Neoproterozoic granitoids from the Axum area, northern Ethiopia. J. Afr. Earth Sci. 27 (3–4), 437–460.

Tadesse, T., (1996). Structure across a possible intra-oceanic suture zone in low-grade Pan-African rocks of northern Ethiopia. Journal of African Earth Sciences 23, 575-381.

Tadesse, T., Suzuki, K., Hoshino, M., (1997). Chemical Th–U total Pb isochron age of zircon from the Mareb Granite in northern Ethiopia. J. Earth Planet. Sci. Negoya Univ. 44, 21–27.

Tadesse T. (1997). Geology of Axum area, Ethiopian Institute of Geological Survey, Addis Ababa, Ethiopia, Memoir No.9.

Tadesse, T., Hoshino, M., Sawada, Y., (1999). Geochemistry of low-grade metavolcanic rocks from the Pan-African of the Axum area, northern Ethiopia. Precambrian Research 99, 101–124.

Tadesse, T., Hoshino, M., Suzuki, K., Iizumi, S., (2000). Sm–Nd, Rb–Sr and Th–U–Pb Zircon ages of syn- and post-tectonic granitoids from the Axum area of northern Ethiopia. Journal of African Earth Sciences 30, 313–327.

Teklay, M. (1997). Petrology, geochemistry and geochronology of Neoproterozoic magmatic arc rocks from Eritrea: implications for crustal evolution in the southern Nubian Shield, Eritrea. Department of mines. Memoir No. 1: 125pp.

Teklay, M., Kröner, A., Mezger, K., and Oberhansli, R., (1998). Geochemistry, Pb-Pb single Zircon ages and Nd-Sr isotope composition of Precambrian rocks from southern and Eastern Ethiopia: implications for crustal evolution in East Africa. Journal of African Earth Sciences, 26, 207-227.

Teklay, M., Kro¨ner, A. & Metzger, K. (2001). Geochemistry, geochronology and isotope geology of Nakfa intrusive rocks, northern Eritrea: products of a tectonically thickened Neoproterozoic arc crust. Journal of African Earth Sciences, 33, 283–301.

Teklay, M., Kröner, A., and Mezger, K., (2002). Enrichment from plume interaction in the generation of Neoproterozoic arc rocks in northern Eritrea: implications for crustal accretion in the southern Arabian-Nubian Shield. Chemical Geology 184, 167-184.

Teklay, M., (2006). Neoproterozoic arc–back–arc system analog to modem arc–back–arc systems: evidence from tholeiite-boninite association, serpentinite mudflows and across-arc geochemical trends in Eritrea, southern Arabian–Nubian Shield. Precambrian Res. 145, 81–92.

Timothy M. Kusky, Mohamed Abdelsalam, Robert J. Stern, Robert D. Tucker, (2003). Evolution of the East African and related orogens, and the assembly of Gondwana. Precambrian Research 123 (2003) 81–85.

Woldehaimanot, B. (2000). Tectonic setting and geochemical characterization of Neoproterozoic volcanics and granitoids from the Adobha Belt, northern Eritrea, Journal of Earth Sciences. 30: 817-831.

Wood, D.A., Joron, J.L., Treuil, M., Norry, M., Tarney, J., (1979). Elemental and Sr isotope variations in basic lavas from Iceland and the surrounding ocean floor: the nature of the mantle source inhomegeneities. Contributions Mineralogy Petrology 70, 319-339.

Yibas, B., Reimold, W.U., Armstrong, R., Koeberl, C., Anhaeusser, C.R., Phillips, D., (2002). The tectonostratigraphy, granitoid geochronology and geological evolution of the Precambrian of southern Ethiopia. Journal of African Earth Sciences 34, 57–84.

LIST OF APPENDIX

Appendix 1: Structural Data

No	Measured structural element	strike	Dip amount and direction	location
1	Foliation (S1)	005	70 SE	0579309E,1532611N
2		015	75 SE	0579140E,1532424N
3		005	80 SE	0578976E,1532479N
4		020	80 SE	0578885E,1532565N
5		010	60 SE	0578578E,1532503N
6		060	50 SE	0576914E,1532612N
7		025	65 SE	0576491E,1532770N
8		020	50 NW	0576218E,1532782N
9		015	80 E	0576055E,1532816N
10		010	45 NW	0576016E,1532833N
11		005	65 NW	0575844E,1532803N
12		340	70 SW	0575773E,1532733N
13		010	55 W	0575683E,1532583N
14		345	50 SW	0575380E,1532620N
15		330	60 SW	0575192E,1532641N
16		350	80 SW	0575119E,1532703N
17		330	60 SW	0574892E,1532725N
18		NS	70 W	0578504E,153033N
19		010	80 SE	0578172E,1530544N
20		NS	80 E	0578048E,1530592N
21		010	70 SE	0577955E,1530582N
22		030	50 SE	0577579E,1530601N
23		010	65 SE	0577378E,1530592N
24		025	80 SE	0576911E,1530592N
25		350	65 NE	0576496E,1530581N
26		020	60 SE	O575918E,1530818N
27		320	50 NE	0575792E,1530852N
28		350	65 NE	0576160E,1531530N
29		NS	50 NE	0575916E,1531574N
30		015	60 SE	0575871E,1531560N
31		NS	65 NW	0575733E,1531617N
32		340	80 SW	0575408E,1531527N
33		350	70 NE	0575170E,1531518N
34		NS	55 EW	0574979E,1531471N
35		010	80 SE	0574719E,1531428N
36		NS	70 EW	0574146E,1531253N
37		020	70 NW	0579040E,1533581N
38		NS	85 SE	0578984E,1533645N
39		045	65 SE	0578497E,1533630N
40		030	78 SE	0577910E, 1533719N
41		NS	70 SE	0576925E,1533674N

42	Foliation (S1)	350	75 NE	0576721E,1533657N
43		010	60 NW	0576526E,1533884N
44		025	75 SE	0576280E,1533684N
45		015	75 SE	0575847E,1533660N
46		NS	75 SE	0575540E,1533617N
47		NS	75 W	0575312E,1533702N
48		010	70NW	0579129E,1535594N
49		005	75SE	0578249E,1535720N
50		015	70SE	0577354E,1536546N
51		010	70SE	0575960E,1536970N
52		NS	65SW	0575303E,1536736N
53		010	75SE	0575298E,1536592N
54		350	60NE	0575035E,1536490N
55		010	80NW	0574459E,1536007N
56		330	55SW	0574462E,1535889N
57		NS	60SW	0575071E,1534531N
58		010	75SE	0578962E,1534190N
59		355	65SW	0578759E,1534512N
60		010	55NW	0578356E,1534619N
61		NS	75SW	0578232E,1534651N
62		005	75NW	0576957E,1534693N
63		335	50SW	0575975E,1534404N
64		NS	70SW	0576244E,1533608N
65		010	80SE	0578943E, 1532618N
66		010	70NW	0575729E,1534156N
67		NS	65SW	0575782E, 1534156N
68		010	75NW	0578748E, 1535596N
69		015	55NW	0577541E, 1535674N
70		NS	70SE	0576959E, 1535640N
71		010	75 NW	0575114E,1535679N
72		NS	65NW	0575405E, 1535459N
1	Joints	330	85NE	0578976E,1532479N
2		290	45NE	0578885E,1532565N
3		060	85SE	0576218E,1532782N
4		E-W	80SE	0576218E,1532782N
5		340	55SW	0576218E,1532782N
6		120	50NE	0576055E,1532816N
7		070	70NW	0575773E, 1532733N
8		340	55NE	0575773E, 1532733N
9		E-W	30S	0575380E, 1532620N
10		080	45NW	0575119E, 1532703N
11		050	65NW	0575119E, 1532703N
12		350	80NE	0577955E,1530582N
13		340	65NE	0577378E,1530592N
14		010	20NW	0577378E,1530592N
15		NS	20SW	0577378E,1530592N
16		005	55SE	0577210E,1530610N
17		020	40NW	0577210E,1530610N

18	Joint	320	80NE	0576911E,1530592N
19		015	25NW	0576911E,1530592N
20		EW	vertical	0576496E,1530581N
21		330	75NE	0576496E,1530581N
22		340	55SW	0576496E,1530581N
23		280	80NE	0575918E, 1530816N
24		030	55SE	0576160E,1531530N
25		060	45NW	0576160E,1531530N
26		260	60NW	0575408E,1531527N
27		EW	60SW	0574979E, 1531471N
28		340	57SW	0574979E, 1531471N
29		050	vertical	0574719E, 1531428N
30		025	30NW	0576721E, 1533657N
31		340	85NE	0576721E, 1533657N
32		350	50SW	0576721E, 1533657N
33		300	75SW	0575312E, 1533702N
34		030	65NW	0574462E, 1535889N
35		250	vertical	0578759E, 1534512N
36		NS	55SW	0578759E, 1534512N
37		230	75SE	0576957E, 1534693N
38		330	35SW	0576957E, 1534693N
39		320	50NE	0575975E, 1534404N
40		290	85SW	0575975E, 1534404N
41		050	40NW	0578943E, 1532618N
42		240	30NW	0578943E, 1532618N
43		050	75SE	0578905E, 1532648N
44		030	25NW	0578905E, 1532648N
45		260	V EW	0575782E, 1534156N
46		340	70SW	0575782E, 1534156N
47		030	65SE	0575782E, 1534156N
48		060	55NW	0578748E, 1535596N
49		055	80SE	0575114E, 1535679N
50		330	55SW	0575114E, 1535679N
	Total	**122**	**122**	

No	Measured structural element	Plunge	Bearing	location
1	Lineation	25	185	0579309E,1532611N
2		70	030	05778578E,1532503N
3		70	005	0576055E,1532816N
4		62	055	0578172E,1530544N
5		60	030	0577955E,1530582N
6		20	175	0577579E,1530601N
7		17	201	0576911E,1530592N
8		14	180	0574719E,1531428N
9		30	180	0578984E,1533643N
10		20	190	0578497E,1533630N
11		25	180	0575312E,1533702N
12		30	191	0575960E,1536970N
13		20	165	0575729E,1533905N

No	Measured structural element	Plunge	Trend	location
1	Fold Axis	20	180	0576218E,1532782N
2		15	170	0576218E,1532782N
3		20	160	0575773E,1532733N
4		15	185	0576496E,1530581N
5		25	170	0575792E,1530852N
6		80	020	0578639E,1531560N
7		25	200	0575733E,1531617N
8		45	050	0574265E,1534297N
9		20	185	0575820E,1533747N
10		15	165	0575852E,1533758N
11		12	178	0575312E,1533702N
12		22	195	0575960E,1536970N
13		63	055	0575729E,1533905N
14		90	-	0578639E, 1530379N
15		14	200 m.room	0575871E, 1531560N
	Total			

No	Measured structural element	strike	Dip amount & direction	location
1	Fold Axial plane	200	80 NW	0576218E,1532782N
2		175	55NE	0576218E,1532782N
3		150	55SW	0575773E,1532733N
4		185	50 NW	0576496E,1530581N
5		200	60NW	0575792E,1530852N
6		030	67SE	0578639E,1531560N
7		230	80 NE	0575733E,1531617N
8		030	70SE	0574265E,1534297N
9		190	65SE	0575820E,1533747N
10		210	45NW	0575852E,1533758N
11		180	30W	0575312E,1533702N
12		200	40NW	0575960E,1536970N
13		050	45SE	0575729E,1533905N
14		000	90	0578639E,1530379N
15		205	70NW	0575871E,1531560N

Appendix 2 Abbreviations

Act	**Actinolite**
Am	Amphibole
Cal	Calcite
Chl	Chlorite
Ep	Epidote
Kfs	K-feldspar
Ms	Muscovite
Ol	Olivine
Pl	Plagioclase
Qtz	Quartz
Ser	Sericite
Tr	Tremolite
MV	Metavolcanic
MVC	Metavolcaniclastics

DECLARATION OF ORIGINALITY

This thesis is my original work and has not been presented for a degree in any other university, and that all sources of material used for the thesis have been duly acknowledged.

Tamrat Mekuria